Detecting Lesions in MRI Brain Images Combining Pseudo-Color Segmentation with Fuzzy C-Means Clustering

Fariba Beiramzadeh Azar

Submitted to the
Institute of Graduate Studies and Research
In partial fulfillment of the requirements for the Degree of

Master of Science
in
Electrical and Electronic Engineering

Eastern Mediterranean University
August 2013
Gazimağusa, North Cyprus

Approval of the Institute of Graduate Studies and Research

Prof. Dr. Elvan Yılmaz
Director

I certify that this thesis satisfies the requirements as a thesis for the degree of Master of Science in Electrical & Electronic Engineering.

Prof. Dr. Aykut Hocanın
Chair, Department of Electrical and Electronic Engineering

We certify that we have read this thesis and that in our opinion, it is fully adequate, in scope and quality, as a thesis of the degree of Master of Science in Electrical and Electronic Engineering.

Assoc. Prof. Dr. Hasan Demirel
Supervisor

Examining Committee

1. Assoc. Prof. Dr. Hasan Demirel _____

2. Assoc. Prof. Dr. Erhan A. İnce _____

3. Assist. Prof. Dr. Rasime Uyguroğlu _____

ABSTRACT

As biomedical image analysis has been improved over the last decades, the widespread advancement of detection/estimation approaches has aided the rapid development of new technologies for monitoring and diagnosis, as well as, treatment of patients. Image segmentation plays a substantial role as part of the preprocessing in various biomedical applications. The segmentation technique is widely used by the radiologists to interpret the input medical image into meaningful data to be used for the extraction of the required features for further processing. Clustering as one of the widely used image segmentation techniques, which can be used in numerous biomedical applications, such as quantification of tissue volumes, diagnosis, study of anatomical structure, and computer-integrated surgery. There is a vast variety of imaging tools such as Magnetic Resonance Imaging (MRI), Computed Tomography (CT), Positron Emission Tomography (PET) and ultra sound in which the segmentation can be utilized.

In this thesis we propose a new approach for tumor detection in magnetic resonance imaging (MRI) brain images, which is utilized by using pseudo-color based segmentation with Fuzzy C-Means clustering (FCM) method. The key idea of pseudo-colored segmentation method with FCM is to segment the given MRI image by converting the prior gray-scale image into a pseudo-colored image and then identify the tumor tissue by using proposed clustering algorithm FCM. The proposed method contains an efficient clustering scheme which can be used in MRI applications.

The application of this method in tumor detection and segmentation could assist pathologist to recognize tumor size and region successfully. The results obtained by

the proposed FCM based approach are very competitive and better in most cases in comparison with the K-Means clustering method, which is one of the important approaches available in the literature for the same problem. FCM based system outperforms the K-Means based system with respect to final segmentation performance evaluated by sensitivity, precision, SSIM, PSNR and segmentation accuracy metrics. The superiority of the FCM based system over the K-Means based system has been verified with the obtained results.

Keywords: Image segmentation, Clustering, K-Means, FCM, medical image processing, brain tumor detection, MRI analysis.

ÖZ

Biyomedikal imge analizi son on yıl içinde gelişme kaydetmiş ve algılama/kestirim yaklaşımlarında yaygın ilerleme sağlayarak hasta izleme ve tanı yanı sıra, hastaların tedavisi için de yeni teknolojilerin hızla gelişmesine destek vermiştir. Görüntü bölütleme çeşitli biyomedikal uygulamalarda ön işlem süreçi olarak önemli bir rol oynamaktadır. Bölütleme tekniği yaygın olarak radyologlar tarafından medikal girdi imgelerinden anlamlı veri çıkarımı ve yorum yapabilme amacıyla kullanılmakta ve çıkarımı yapılan verilere daha sonraki süreçlerde gereksinim duyulmaktadır. Kümeleme birçok biyomedikal uygulamalarda yaygın olarak kullanılabilen bir görüntü bölütleme tekniği olarak değerlendirilebilir. Bahse konu uygulamalar arasında doku hacmi niceleme, tanı koyma, anatomik yapı değerlendirme, ve bilgisayar destekli cerrahi sayılabilir. Ayrıca, Manyetik Resonans görüntüleme (MRI), Bilgisayarlı Tomografi (CT), Pozitron Emisyon Tomografi (PET) ve ultra ses görüntüleme gibi çok çeşitli araçlarda bölütleme uygulamaları kullanılmaktadır.

Bu tezde, bulanık c-ortalama (FCM) kümeleme ile sözde-renkli bölütleme yöntemlerini kullanan manyetik rezonans görüntüleme (MRI) tabanlı beyin görüntülerinde tümör tespiti gerçekleştirebilen yeni bir yaklaşım öneriyoruz. FCM ile sözde-renkli bölümleme yöntemlerini kullanmadaki en önemli ve anahtar fikir eldeki gri-tonlu MRI girdi imgesinin sözde-renkli bir imgeye dörüştürüldükten sonra önerilen FCM kümeleme algoritması yordamı ile tümör dokusunun belirlenmesi ve bölütlenmesidir. Önerilen yöntem, MRI uygulamalarında rahatlıkla kullanılabilecek önemli bir yaklaşımdır. Bu tümör tespit ve bölütleme yönteminin uygulanması patologlara başarılı bir şekilde tümör boyutu ve bölgesinin balirlenmesinde yardımcı olabilir. Önerilen FCM dayalı bir yaklaşım ile elde edilen sonuçlar, literatürde

mevcut olan önemli yaklaşımlardan biri olan K-ortalama yöntemi ile karşılaştırıldığında pek çok durumda daha rekabetçi ve başarılı sonuçlar elde edilmiştir. FCM tabanlı sistem ile K-ortalama tabanlı sistem ile sonuçta elde edilen bölütleme performasları duyarlılık, hassasiyet, SSIM, PSNR ve belütleme doğruluğu metrikleri bağlamında karşılaştırılmış ve FCM tabanlı sistemin üstünlüğü doğrulanmıştır.

Anahtar Kelimeler: Görüntü bölütleme, kümeleme, K-Araçları, FCM, tıbbi görüntü işleme, beyin tümörü tespit, MRI analizi.

DEDICATION

This dissertation is dedicated to my lovely parents for their love, devoting their time to support me. Further, I would like to dedicate this work to my beloved husband for his encouragement and endless support.

ACKNOWLEDGMENTS

I would like to thank Asst. Prof. Dr. Hasan Demirel for his continuous support and guidance in the preparation of this study. Without his invaluable supervision, all my efforts could have been short-sighted.

Prof. Dr. Aykut Hocanın, Chairman of the Department of Electrical & Electronic Engineering, Eastern Mediterranean University, helped me with various issues during the thesis and I am grateful to him. Besides, a number of friends had always been around to support me morally. I would like to thank them as well.

I owe quit a lot to my family specially my husband who allowed me to travel all the way from Iran to Cyprus and supported me all throughout my studies. I would like to dedicate this study to them as an indication of their significance in this study as well as in my life.

TABLE OF CONTENTS

LIST OF TABLES

LIST OF FIGURES

LIST OF SYMBOLS/ABBREVIATIONS

ΔE	Chromatism in CIELa*b* space
A	Positive definite $n \times n$ Matrix
a_l	Eigen value set
a*	Color channel of CIELa*b*
b*	Color channel of CIELa*b*
C	Number of Cluster
C_{pq}	Similarity measure between two nodes, pand q
c_j	Center Vector
D	Sum of costs of node
D_x	Diagonal element
d_{ij}	Euclidean distance measure
F	Input image
G	Segmented image, gray level of pixel
H	Hue Component
I	Identity matrix
I	Center of cluster
J	Objective function
L	Luminocity
M_A	Average of gray value of A
M_B	Average of gray value of B
M	Weighting exponent on each fuzzy membership

N	Number of cluster
R^n	N dimensional R space
T	Threshold
T_0	Initial Threshold
T_n	n^{th} Threshold
T1w	Tissue value –weighted
$U^{(k)}, U^{(k+1)}$	Optimal matrix norm
V_i	Distance of k data from cluster centers
W	Cost matrix
X	Input Dataset
X_j	Data point
x_i	Membership within i^{th} cluster
$\| \ \|_{\Lambda}$	Induced A-Norm
$\left\|x_i - c_j\right\|$	Distance between object and cluster center
$\langle X, Y \rangle$	Inner product function between X and Y
CIE	Comission International de l'eclairage
CT	Computed Tomography
CSF	Cerebrospinal Fluid
DCT	Discrete Cosine Transform
JPEG	Joint Photographic Expert Group
FCM	Fuzzy C-Means
FN	False Positive
MR	Mgnetic Resonance

MRI	Magnetic Resonance Imaging
MSE	Mean Square Error
PET	Positron Emission Tomography
PD	Proton Density
PSNR	Peak Signal to Noise Ratio
RGB	Red,Green,Blue
ROC	Receiver Operating Characteristic
SSIM	Structural Similarity Index Measurement
TN	True Negative
TP	True Positive

Chapter 1

INTRODUCTION

In last couple of years, revolutionary progress in radiological science betrays the importance of image processing in clinical diagnostic affairs. A number of medical instruments in diagnosis, evaluation and treatment of mortal disease have been invented. The common target of whole these tools is to design an efficient segmentation algorithm. Additionally many image processing and analysis methods are improving to have better understanding images which could assist to make accurate and on time decisions. Some medical imaging methods are X-ray CT (Computed Tomography), Magnetic Resonance Imaging (MRI), PET (Positron Emission Tomography) and Ultrasound. Generally all these methods use computerized automation to process of digital images. As a consequence, multidimensional images can be analyzed to illustrate characteristic features by computers [1] [2].

Medical images mostly contain some specific characteristics such as noise, inhomogeneity and other complicated features. So, medical image segmentation may seem to be a defiant and sophisticated process. Fortunately medical imaging has a benign capacity to do research on it. Although many segmentation algorithms have been proposed up to now, honestly none of them can cover a generic successful segmentation algorithm in medical images. Medical images can depict the function

of each organs or the behavior of various organs in the treatment duration as well as an interpreter [2] [3].

Because of the advantages of magnetic resonance imaging over other diagnostic imaging methods, the most researches in medical image segmentation employ MR images. Magnetic Resonance Imaging provides anatomical soft tissue information of human body. It displays pure details and requires no radiation gleam such as what is used within X-ray imaging method. It is excessively flexible method since a contrast between one tissue and other, can be changed by altering the way of imaging. For instance by changing the radio frequency and gradient pulses it is possible to produce images with high contrast. In particular, as a task of involving with anatomical structures, MR imaging, has different biomedical imaging applications such as characterization of tissue volumes, diagnosis and study of human organ and etc. There are different approaches in multi parameters MRI data such as maximum contrast methods artificial neural networks, clustering technique, Eigen image filtering and optimal feature space, all can be obtained in tissue segmentation. In this thesis the chosen approach is clustering method [4].

Recently brain segmentation in MR imaging has become very challenging issue in medical. Image segmentation holds a prominent role in brain image processing significantly. The influence of image segmentation has been clearly highlighted in this specific medical environment where the abrupt pre-surgery and post-surgery decisions are required to take in order to save time and speed up the recovery process. Magnetic resonance (MR) image has become more and more important in research and clinical tasks including in pathology, pre-surgical planning and even in computer integrated surgery. Brain MR Image can successfully assist medicines in

pre-surgical planning and early recognition consequently leads to eradicate unwanted and perilous light-speed spread diseases like brain tumors. In addition, automated image segmentation could thoroughly enable radiologists to immediate detect abnormal changes in tissues or organs rather than manual image segmentation, which is unexpectedly a sort of time-consuming process. It is the prerequisite for quantitative morph-metric analysis, 3-dimension volume visualization and structure-function correlation measurement using MRI images. A common segmentation sort of brain MRI is the process of labeling pixels with respect to their tissue type consisting of White Matter (WM), Grey Matter (GM), Cerebrospinal Fluid (CSF) and particularly pathological tissues like tumor and edema. However, there are some problems in tissue classification. Mainly MR images are sensitive to parameters like imaging features of scanners, and then a segmentation algorithm could not distinguish between intensities and tissues subsequently leads to reveal great overlaps of intensity ranges among different tissues. The other problem is in-homogeneity of magnetic field and biological fluctuation in different structures in one single cluster. And the last problem is a partial volume effects caused to have a blurred tissue boundary. So the intensity-based algorithms could not classify MR images efficiently [5] [6] [7].

To overcome these problems we suggested a method called Fuzzy C-Means algorithm, which not only can take intensity feature of MR brain images but also it holds morphological characteristics. Results in chapter 7 could easily show the considerable advantages of FCM algorithm.

In this thesis, a tumor tracking algorithm will be proposed which will utilize pseudo-colored segmentation with Fuzzy C-Means clustering in MRI brain lesion namely are

tumors or edemas. This method would assist radiologist to recognize exact size and region of lesion as well.

1.1 Thesis Contributions

FCM is used as an alternative clustering algorithm for segmentation of tumors in the MRI based brain images

- The segmentation performance of the FCM based brain tumor segmentation is analysed and it superiority over the widely used K-Means clustering based segmentation is shown.
- The effect of clustering parameters, such as number of clusters required, on the final segmentation accuracy is studied for determining such parameter values for possible MRI tumor detection application.
- The segmentation performance is not only studied by subjective evaluation such as visual inspection, but also extensively analysed by using objective segmentation performance analysis metrics including: sensitivity, precision, SSIM, PSNR and segmentation accuracy.

1.2 Thesis Overview

Chapter 1 as an introduction includes brief review of medical image and explaining main problem in MR images segmentation, propose a solution proved by results after applying proposed method. Chapter 2 deals with definition of segmentation, segmentation application in medical image processing. Chapter 3 is discussing clustering technique and different types of clustering methods, introducing standard methods called K-Means with its mathematical formulations, and describing its typical applications. Chapter 4 contains a definition of FCM algorithm and its applications in medical images, describing its advantages in comparison with K-Means clustering. Chapter 5 gives an instructions to generate pseudo-coloring

method, debating gray-scale to RGB, RGB to HSI, HSI to La*b* color space transformations formulas. In Chapter 6 we explained the implementation of our used K-Means and FCM segmentation methods in details including block diagrams, which show the process clearly. In chapter 7 there are experimental results for some test cases after obtaining both methods. The comparison between two cases have been observed and shown in tables and graphs obviously. Finally in chapter 8 we will come to conclusion by taking decision based on results and suggest more effective and accurate method for future works in medical science.

Chapter 2

IMAGE SEGMENTATION

Segmentation holds a crucial role in analysis and recognition of an image in digital image processing. Image segmentation can be utilized in diverse applications with different purposes. Some popular acquisitions are object detection processes like face detection, pedestrian detection and brake light detection or recognition tasks such as face and fingerprint recognition, machine vision, traffic control systems. Image segmentation more often used in medical science to study of anatomical structures or measure tissue volumes. It is capable of diagnosis abnormal organs in human body. The most important task is to detect and locate tumors and other pathologies in every organ, especially in brain. The tumor region in brain can be seen easily as a result of segmentation. To understand better, the first step is to know what exactly segmentation is.

Image segmentation divides an image into parts, which have correlation with areas or objects in real world [8]. A complete segmentation classifies an image into non overlapping regions that corresponds to objects like what you can see in figure 2.1, all the parts of image are segmented including tiger body and what is around it, while a partial segmentation divides an image into separate homogenous regions with respect to specific features like color, intensity, texture, brightness and etc. Figure 2.2, just grass in image is segmented.

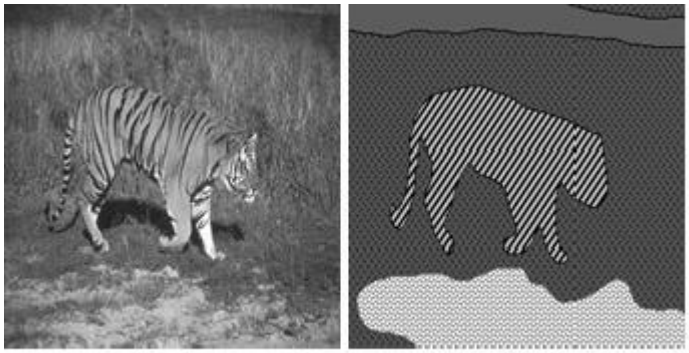

Figure 2. 1:a) Lion Image, b) Complete segmented Image [9]

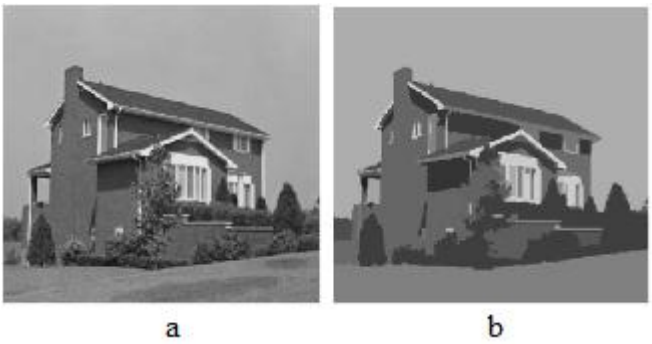

Figure 2. 2: a) House Image,b) Partial Segmented Image [9]

In another word, process of image segmentation is to partition an image to a set of disjoint segments with respect to the pixels with uniform and homogeneous attributes such as intensity, color, tone or texture etc. The aim of segmentation is to simplify an image to some meaningful region, which is easy to be analyzed. The outcome is a collection of segments combined to cover the primary image or a contour, which highlights an important part of an image. In image segmentation the big aim is to detect and extract desired region. The desired region may be any object in image related to type of required applications. These applications might consist of object-recognition, image editing, image compression and etc. The higher quality of digital image correspond better segmentation. Simple images segmentation process seems to be a very clear and effective process dealing with small pixel fluctuation whereas in

complicated images achieving subsequent processing would be challenging or even complex [10].

Image segmentation can be classified in three categories with respect to which, component of image is desired to be segmented. Edge- based segmentation, in which edge data is applied for boundaries of objects. Boundaries can be processed and optimized if necessary, then make a close region with an object within Pixel-based direct segmentation in which histogram statistics of the image give the estimation used in forming close region with an object inside it. Region-based segmentation approach, in where pixels directly are studied for a region growing process according to a pre-defined similarity rules to form close region with an object inside it. After defining the regions, features can be obtained for characterization, classification and finally analysis. The features will contain shape and texture information of each region as well as statistical features such as mean and variance of gray levels [11].

As mentioned before, there are many segmentation algorithms but there is not a general algorithm for mostly effective segmentation of medical images. Some of these algorithms mainly are known as thresholding, compression based methods, histogram based methods, graph based methods, edge detection, region growing methods, clustering methods and etc. Here some popular segmentation algorithms will be discussing briefly [11].

2.1 Thresholding

Thresholding is a simple approach generally used in image segmentation. By using histogram statistics it can convert an input gray level image to single or multiple thresholds. To exempt a threshold for classifying image components into classes it is required to analyze the histogram. If histogram is bimodal, when histogram of an image consists of two dominant modes, the unique threshold can be assigned to gray

space values pointing out the deepest point in histogram valley [7]. If the image is not bimodal the key idea is to partition the histogram into multiple thresholds. Suppose $f(x,y)$ is an image, which has to be segmented in two classes applying a gray space threshold T then:

$$g(x,y)=\begin{cases}1 & if \quad f(x,y)>T\\ 0 & if \quad f(x,y)\le T\end{cases} \tag{2.1}$$

Where $g(x,y)$ is a segmented image, with two classes of binary gray scales 1 & 0 and T is the threshold carried out from histogram. This formula is effective when, image is bimodal in other cases following the basic global thresholding can release the multiple thresholds [12].

1. Define a prior estimated value for $T=T_0$.
2. Segment initial image by T_0. This step divides the pixels into two groups for example A and B. A includes gray level values which are higher than T_0 and B includes gray level values which are equal or less than T_0.
3. Calculate the averages for gray level values of each group, *A* and *B*, giving name for two averages, M_A and M_B.
4. Compute the new threshold:

$$T_n=\frac{M_A+M_B}{2} \tag{2.2}$$

5. Repeat steps 2 and 4 till difference in T_n in best iterations is less than initial value T_0 .

Figure 2.3, is a smple bimodal image as you can see the histogram of image in Figure 2.4 while Figure 2.5 is not a bimodal image by its histogram shows in Figure 2.6.

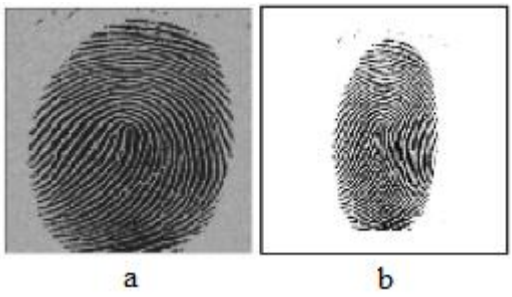

Figure 2. 3: a) Bimodal finger print,b) Segmented image using Thresholding [12]

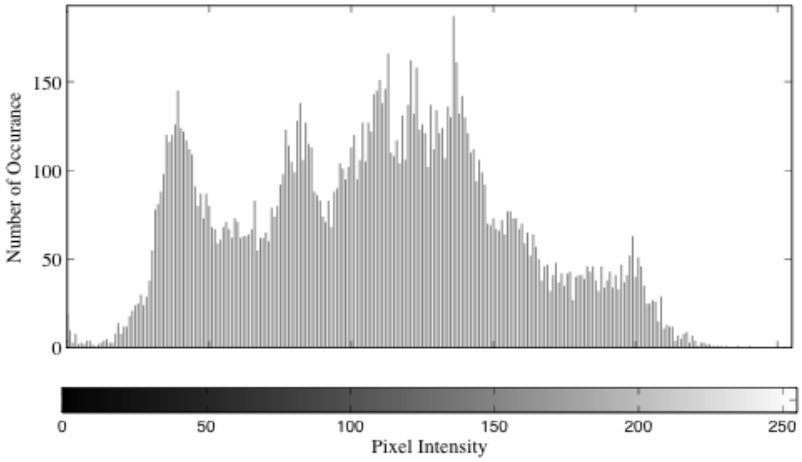

Figure 2. 4: Histogram of Image Finger points

Figure 2. 5: a) Original Lena, b) Segmented Lena using Thresholding [12]

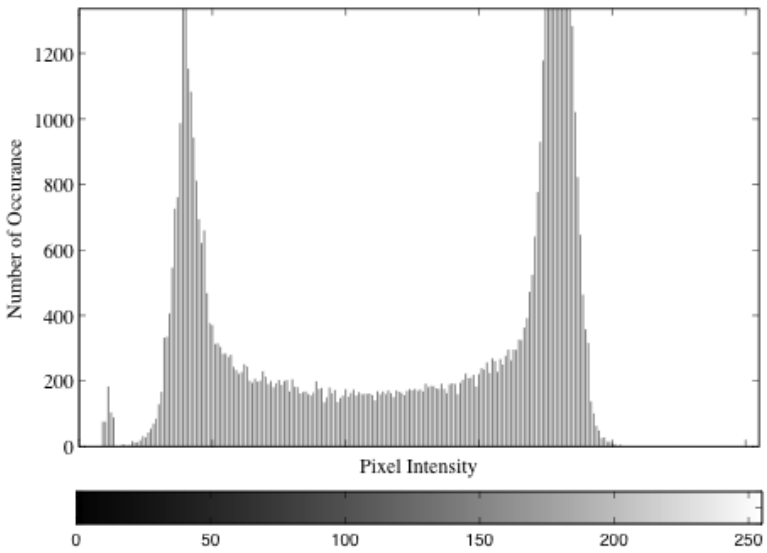

Figure 2. 6: Histogram of Lena

2.2 Compression-Based Segmentation

Compression in image segmentation means to find an optimal segmentation, which minimizes the length of codes coming from data set. Compression has been obtained in order to save transformation bandwidth. It attempts to find a regular pattern in image lead to compress the image by encoding and decoding process. Segments can be defined by means of boundary shapes and textures. Two common types of image compression are Disceret Cosine Transform (DCT)-based methods used to achieve JPEG (Joint Photographic Expert Group) images and wavelet-based methods, which lead to have JPEG2000 images. A compression-based segmentation generally consists of two important blocks called encoder and decoder blocks. In general sample encoder and decoder blocks contain following processes [10].

a) Encod

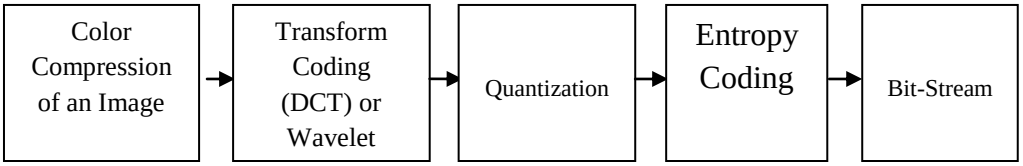

Figure 2. 7: An Encoder Block Diagram [10]

b) Decoder

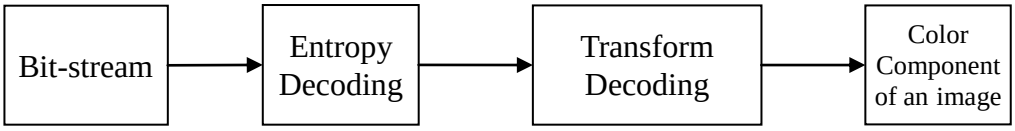

Figure 2. 8: A Decoder Block Diagram [10]

The typical compression based segmentation model can be seen:

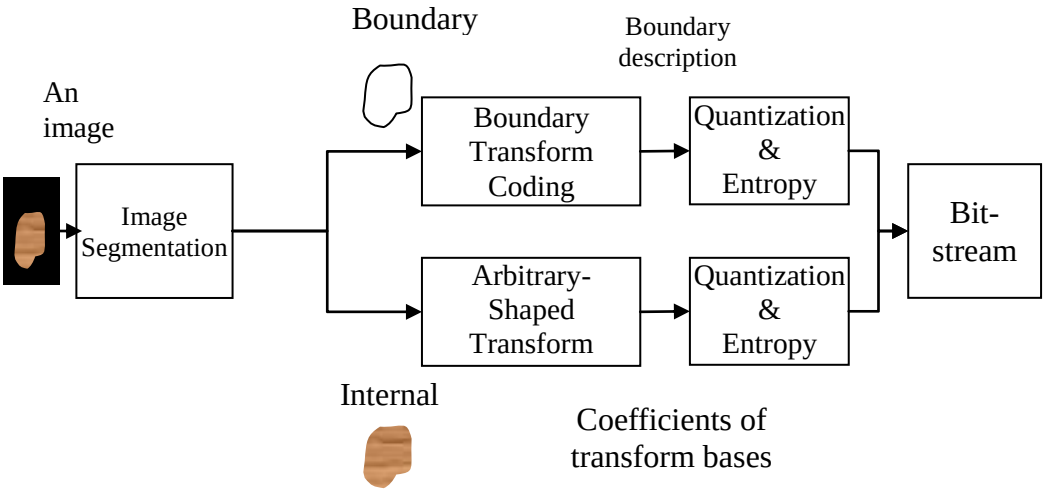

Figure 2. 9: Compression based Segmentation model [10]

There is an image of different fruits applying compression-based segmentation resulted emerging three different regions of interest of image in Figure 2.10.

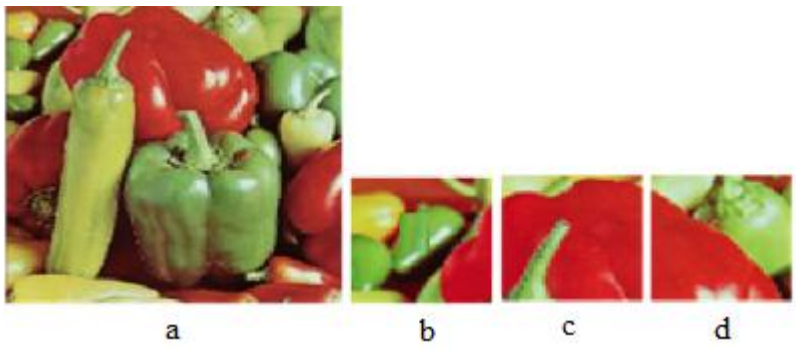

Figure 2. 10: a) Original Vegetables, b, c, d) Segmented parts of image using compression based segmentation [10]

Actually the target of compression is to find the segmentation, which produces the shortest coding length among other possible segmentations. It can be achieved within

a clustering method. The rate of loss compression identifies the coarseness of the segmentation in which optimal value normally varies for each image. Mentioned parameter can be easily estimated from the contrast of textures in an image. For instance, when the textures in an image are similar, it needs stronger sensitivity and lower quantization.

2.3 Histogram-Based Segmentation

In histogram technique, all peak and valley points in histogram computed from all pixels in an image can be classified into several clusters with respect to pixel features like color or intensity. Unlike other segmentation methods it requires one pass through pixels then it is more effective and favorable. This efficiency motivates the technique to be applied in multiple frames. For instance, applying this segmentation on active points can lead to reveal a various type of segmentation called video tracking. On the other hand, it may not be capable to distinguish specific peak or valley points in some images. Figure 2.11, illustrates lady's skin color segmentation based on a kind of histogram based method [12].

Figure 2. 11: a) lady image,b) segmented color skin using histogram-based segmentation [12]

2.4 Edge Detection for Segmentation

Edge detection is very important field in image segmentation. Edges can represent the intensity changes in an image. Edges normally appear between two different

regions by defining the boundaries. The main idea is to extract some important or desired attributes of an image. Edge as a major feature for an image can indicate the high frequency as well. Detecting edges in an image can ease object recognition, data compression and finally image segmentation. Since edges and noises both have high frequencies then edge detection may be a kind of problematic process in noisy images [13]. Other possible problems may be edge localization, missing true edges and high computational time. To reach high accuracy and low noise the great deal is to define appropriate threshold values to the image operators. According to Hoffman and Jain [14] there are three edge types in images: step edges, roof edges and smooth edges. The step edges, refers to edges made of pixels which show significant depth differences in comparison with their neighborhood. Roof edges imply wide differences in normal orientation. Smooth edges are associated togradual and smooth variations in normal orientation.Olga has tried to propose an enhanced range image segmentation method with information of objects from edge detection by clustering algorithm [14]. In this paper, the author used thining, closeing and erosion methods to solve problems in edge detection. To have precise edges with low noise thinning process is employed while false small regions composed by closing process is destroyed within growing process. And finally erosion can produce a set of pixels to choose initial values. Figure 2.12 clearly shows the process of segmentation based on edge detection. As you can see, a is a step edge of input image, b is a range image, c is a roof edge of given image, d is a raw edge map of image, e is result of edge closing process, f is result of edge thininig, g is a segmented image using Region growing method,h is a segmented image after erosion and finally i is a segmented image after using edge detection according their proposed method.

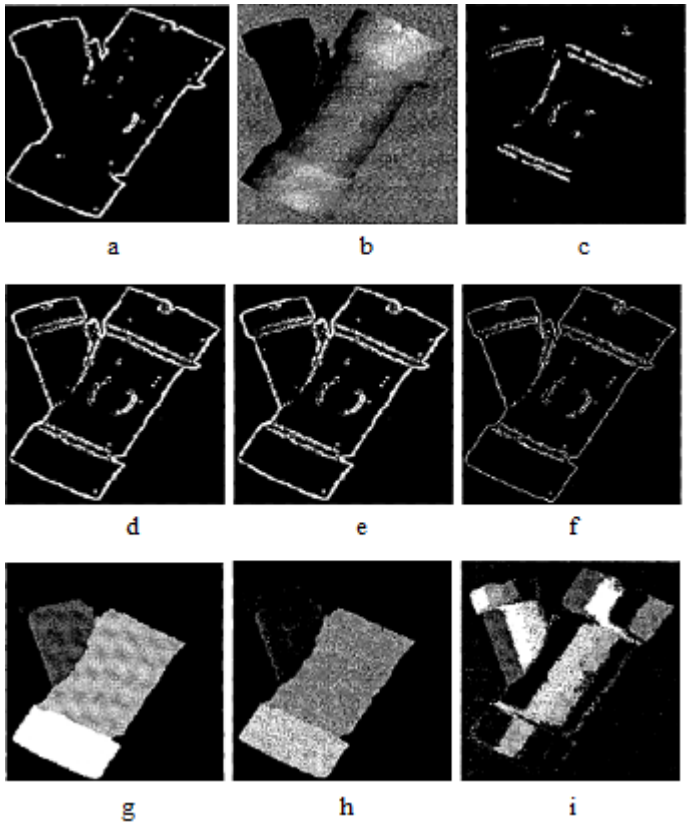

Figure 2. 12: a)Step Edge, b) Range Image, c) Roof Edge, d)Raw EdgeMap, e) Edge Closing, f) Edge Thining, g)Region Growing, h) Region Grwing with Erosion, i)Segmented imge using Edge Detection [14]

2.5 Region Growing Methods

In this technique all pixels can be assembled to form specific regions with respect to their similar features. The region growing methods employ some seeds in order to extract the object, which is required to be segmented. Choosing of seeds directly affect to final result of region growing segmentation process. On the other hand noise in image caused to assign wrong seeds. The technique starts with selecting a seed and subsequently region grows around this seed. After region growing is finished, the next step is to choose the other seed from untagged pixels then the next region growing is going on [15]. There are some important issues which are must be considered in this method such as selecting the right pixels as a set of seeds to

represent the chosen region, defining specific criteria for region growing algorithm to spread in neighbor pixels, put appropriate limit for technique to be stopped in right time. According to [16] region growing method is used to detect tumor in small animal PET based on gradient magnitud. Figure 2.13 shows an animal PET Image with tumor and heart. B is a segmented image using ordinary region growing method and c is a segmented image using proposed region growing mehod by Oleg.

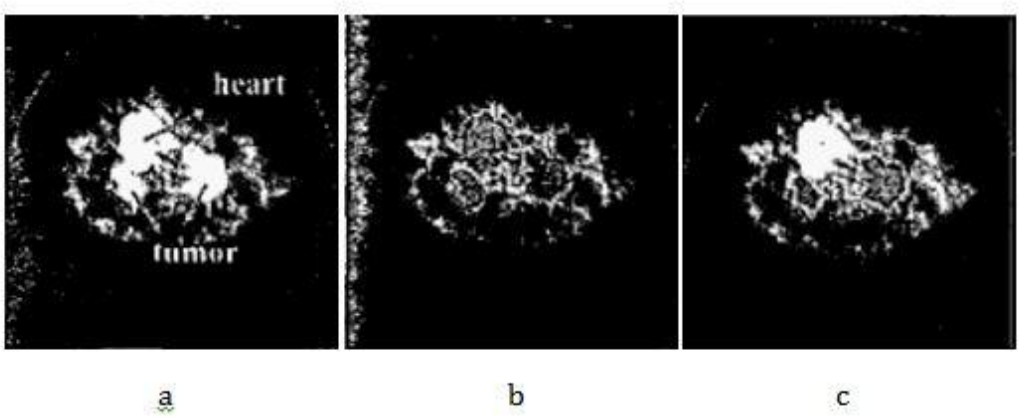

Figure 2. 13: a) Original image including heart and Tumor, b) Segmented image using ordinary region growing , c) segmented image using proposed region growing [16]

2.6 Graph-Based Methods

The basic concept in this method is to determine edges in graph where each pixel considered as a node in it. The weighted edges are remarking the dissimilarity between pixels, in an image. The technique adaptively can design a criterion to classify the whole graph to desired clusters. The output classified pixels or nodes illustrate the segmented object in image. There are several methods obtaining graph segmentation algorithm to segment images. Some popular methods are Random Walker method Normalized Cut clustering minimum cut method, isoperimetric partitioning and minimum spanning tree segmentation. Following sample show an image segmented using graph based segmentation Figure 2.14 [17].

In this figure a shows the original image of sportsmen and b shows the segmented image using grapg-based method.

Figure 2. 14: Sportsmen, b) segmented image using Graph-based segmentation [17]

Chapter 3

CLUSTERING BASED SEGMENTATION

Images may contain many objects more than one object then dividing all objects in segments and find a meaningful point may be a big calamity. Subsequently segmentation can be achieved by clustering. Clustering is a computational tool that tries to find structures or specific patterns in a data set where objects in each cluster have a certain degree of membership. In another word, clustering is a process of dividing object (pixel) into groups based on its features. Therefore, a cluster is a set of similar objects (pixels), which they are totally different from objects belonging to other clusters. Generally clustering algorithms can be classified in two groups, hard clustering algorithm and soft clustering algorithm. In hard clustering methods data partitions to specific clusters and each data point belongs to just one cluster wherese soft clustering algorithm is responsible to associate membership levels and consequently locate each data points in one or more clusters [11].

This sample can simply summarize the clustering process. Clearly, it can be seen how the given data segmented into three clusters identifies by three different colors Red, Blue and Green.

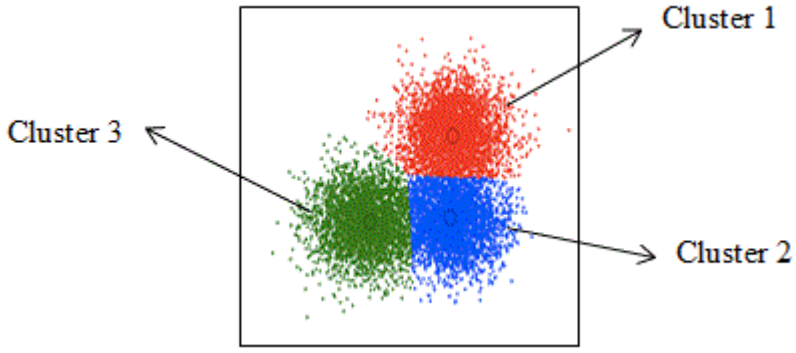

Figure 3. 1: Three Clusters of given

An image might be grouped based on some features like keyword and content of image. Keyword based clustering is to assign a font which describes an image. A keyword represents different attributes of image. Each attribute has a specific value so then similar keywords with same values can be form a cluster together. One of the keyword based techniques is relevance feedback algorithm .In content based clustering content represents every information herd from image such as text or shape. The algorithm or tool, which applies statistical formulas, or pattern recognition or etc called content-based clustering method. The most popular example technique is K-Means clustering which uses pattern recognition to classify images. The mentioned example techniques will be discussed fully later [18].

Also, Clustering method can be divided into supervised-clustering, in which clustering region can be defined manually and unsupervised-clustering that clustering criteria already defined automatically. There are numerous clustering techniques have been used in image segmentation. The first technique, which was mentioned before, is relevance feedback clustering.

3.1 Relevance Feedback Clustering

Relevance feedback as a sort of supervised clustering used to refine desired query based on low-level attributes automatically according to prior evaluation derived by

user validation of the relevance of images. When the relevance feedback sytem distinguish a similarity in a set of images, system continue to refine the query using the most relevant image, which already can be chosen manualy by a user. Relevance feedback is a keyword based image retrieval, which compares input keyword with other images of dataset. If an image has no sufficient keyword to be compared, then image segmentation may seem to be very challenging process. A relevance feedback can overcome current problem as well [19]. The technique utilizes user relevance feedback in order to avoid abrupt errors and general redundancy [20]. Using Bayesian classifier, a relevance feedback method contains both negative and positive feedbacks due to its static nature [11] wherese other content based clustering methods can not be accustomed to user changes [21].

3.2 Log Based Clustering Algorithms

In this technique images can be clustered based on the retrieval system logs followed by an information retrieval process [11]. The current process leads to emerge a session keys which are required for retieval. Clusters can be created through along the sessions. In each session a cluster generates log-based document that maintains similarity of image. Each session has a Log-based vector according to the recieved log-based documents [19]. This vector can change the session cluster. The document which can not be found generally creates its session vector by itself.

Subsequently a hybrid matrix may generate one individual document vector at least with one corresponding log-based vector. The outcome is to achieve a clustered hybrid matrix. In multi-dimensional images this technique is encountered with a big hardship [22].

3.3 Hierarchical Clustering Methods

Hierarchical clustering as a member of clustering algorithms family attempts to construct seeded clusters. When images are multidimensional hierarchical clustering can be a good choice [11]. The hierarchical clusters remind a tree. The unite cluster represents as a root of tree which associates whole data points. Each leave contains a cluster and its unique point [23].

A hierarchical clustering carried out via ward object function, which employs variance reduction approach namely is Ward algorithm. In fact this method is one of the well-known technologies in information retrieval. It is the process of integrate variety images and depict them as unified cluster in a tree shape and subsequently developing a small cluster via chronological steps [11].

Each step is proceeding by minimizing the differences between all leaves (clusters) of a tree. The hierarchical algorithm can apply to measure large number of data points by jointly employing a connectivity matrix to it. However its computation process would be a sort of time-consuming and expensive process. Regardless to connectivity constraints in each step, it emerges all possible merges successfully [24].

The hierarchical clustering can achieve by classifying different image data into x sorts. Simply it classifies all different images and maintains them in a matrix form iteratively in order to conclude cluster centers within their dissimilarity measures. The process could be accessed throw steps are as follows:

1. Figure out similarity scale between initial image and retrieved image.
2. Indicate similarity between two neighbors.
3. Unify them into one single cluster [11].

Here in Figure 3.2, there is a sample image segmented using hierarchical clustering in it. It obviously divides a man image into three seeds and each time tires to pointing out one cluster in imag.

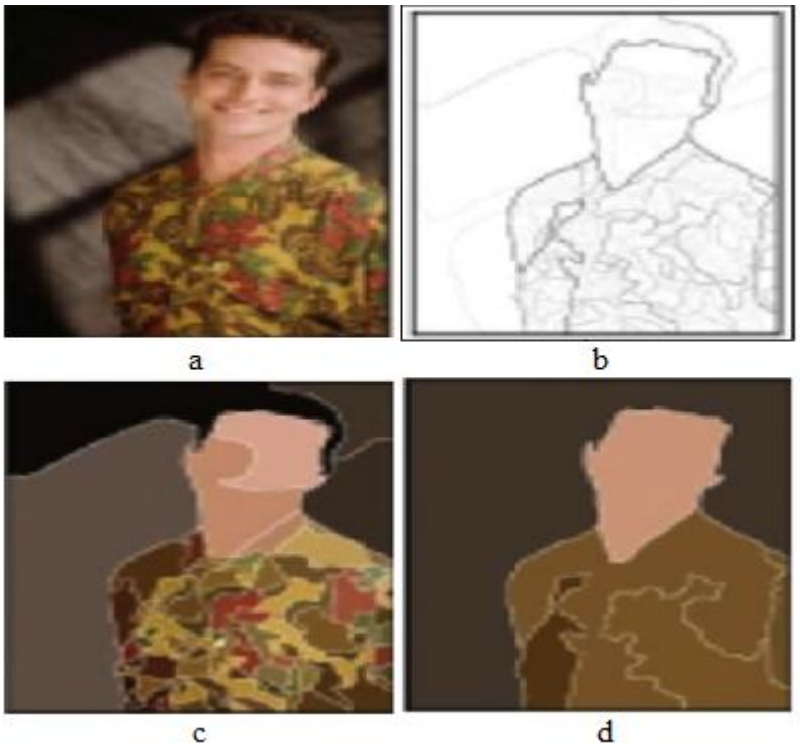

Figure 3. 2 : a) original man mage, b, c, d) 3 different seeds of segmented image [24]

3.4 Retrieval Dictionary Based Clustering

Retrieval Dictionary Based clustering method is a conten-based technique used in image segmentation. This method is performed measuring the distance between two patterns which are classified into different clusters by means of a retrieval stage. The big deal in this system is the determination of calculated distance. Fortunately retrieval dictionary based clustering can overcome the current problem easily [25]. This technique obtains a retrieval dictionary generation block, which is tried to partition mentioned patterns into several clusters lead to come out a retrieval dictionary. In this method, an input image is retrieved according to the distance between two spheres with different radii. Each radius holds a similarity scale

between central cluster and a given image. An image which contains a similar feature in comparison with query image will be retrieved using retrieval dictionary [11].

3.5 Normalized Cuts Algorithm

The main goal in this algorithm is first to detect significant groups then to focus on other small fluctuation and objects in next steps. The advantage of current method is to uniform all different features of an image such as color, intensity, texture and etc into one unite frame. It proposes a graph-based criterion to measure a partition quality of an image. This criterion may conclude in a general Eigen value problem. To overcome this problem it is crucial to define a precise criterion for high quality partition and to know the effective way of desired partition. The mentioned purpose may be achieved by following the chronological steps [26].

1. Imagine an image as a fully connected graph (shown in example), assign a node for each pixel, connect every node (pixels) with a line, give a cost for each line *p* and *q* are two nodes in example and the line which connect these two nodes is their corresponding cost C_{pq} . Actually C_{pq} here measures the similarity between two nodes. Similarity can be computed when the difference in defined features occurs between two nodes. Similar pixels gather in same segments and dissimilar pixels in different segments.
2. Classify graphs into segments (cuts): Clean overlapped line. Clean low-cost lines.
3. Connect cuts:

Cost of cuts can be computed by this formula:

$$aut(A,B) = \sum_{p \in A, q \in B} C_{p,q} \tag{3.1}$$

Now the minimum cut has found out the efficient solution has been reached to overcome the problem but in some cases the minimum cut cannot be a good solution. So, normalized cutsm has been suggested in special cases.

Perceptually normalized cuts method tries to assemble nodes into groups in which amongst groups there is similarity and outside groups there are dissimilarity. This method is empirically shown to be relatively robust in image segmentation [27]. It can be recursively applied to get more than two clusters. Each time the sub graph with maximum number of nodes is partitioned (random selection for tie breaking). The process terminates when the bound on the number of clusters is reached or the Normalized cut value exceeds some threshold T. Nonetheless, the tree organization here may mislead a user because there is no guarantee of any correspondence between the tree and the semantic structure of images. Furthermore, organizing image clusters into a tree structure will significantly complicate the user interface. Normalized cut formula will be:

$$cut(A,B) = \frac{cut(A,B)}{Volume(A)} + \frac{cut(A,B)}{Volume(B)} \tag{3.2}$$

Volume of *A* or *B* can be computed by:

Volume(A)=Sum of costs of all edges around A (3.3)

In matrix form normalized cut will include these steps:

1. Suppose *W* is a cost matrix:

$$W(i,j) = C_{i,j} \tag{3.4}$$

2. Consider *D* as the sum of costs for node I:

$$D(i,j) = \sum_j W(i.j)\,; \quad D(i,j) = 0 \tag{3.5}$$

3. Compute *N-cut* by this formula:

$$Ncut\ (A,B) = \frac{y_T (D-W) y}{y_T D y} \quad ; \quad y_i \in \{1, -b\}\ ,\ y_T D_1 = 0 \tag{3.6}$$

4. Solution can be achieved by means of solving generalized Eigen-value problem:

$$y(D-W) = \lambda D y \tag{3.7}$$

Figure 3.3 shows an original image of sportsmen and b, c, d show the different part of image segmented using *Ncut* segmentation method.

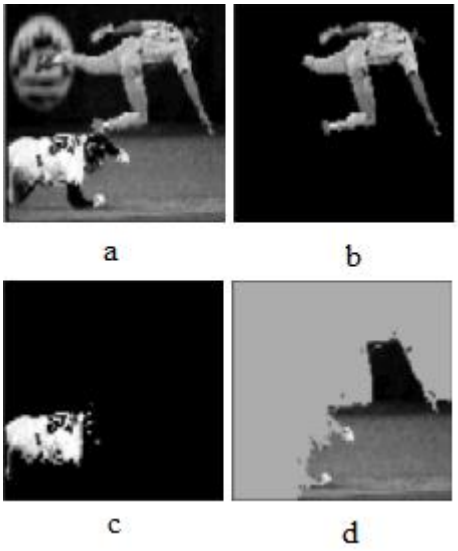

Figure 3. 3: A sprotsmen image segmented by Ncut algorithm [26]

3.6 K-Means Clustering Algorithm

K-Means algorithm is a very popular method used to segment the image to K clusters. Had been invented by Macqueen in 1967, it is one of unsupervised algorithm that can overcome the typical clustering problem in image segmentation. The process consists of a simple and easy steps to divide a given image data into a definite number of clusters. The key idea is to assign K centroids to each cluster. Since different locations cause different results, centroids should have located in trickery way so then it would better to place them as much as possible away from

each other. Former step is to get points one by one belonging to data set and put it in a nearest centroid. This step is completed successfully until no more point has been left. As a result, an early group age emerges out. In this moment only thing is to re-calculate K new centroids as a bar centers of clusters concluded from first process. When K new centroids appear the newer calculation has to be done among pervious data set points and other new nearest centroid. As this loop persists on, the K centroids change their places step by step till no more changes have been seen [5].

Employing K-Means clustering algorithm may illustrate a certain number of nonhierarchical or flat and disjoint clusters. Though, it is appropriate to generate global clusters since it is an unsupervised, non-deterministic, numerical and iterative method. In another word, data vectors in K-Means method are divided into predefined and known number of clusters [22] [28]. At the beginning the centroids (mean) of the predefined clusters are initialized randomly. The dimensions of the centroids are same as the dimension of the data vectors. Each pixel is assigned to the cluster based on the closeness, which is calculated by the Euclidian distance measure when all pixels are clustered, the mean of each cluster is recalculated [29]. This process is repeated until no significant changes result for each cluster mean or for some fixed number of iterations.

K-Means algorithm typically consists of following steps:

1. Choosing the k number of clustering manually or randomly $v_i \quad , \quad i = \{1, 2, \ldots k\}$.
2. Generating k clusters by assigning each point x_j to nearest cluster mean v_i using Euclidean distance measurement:

$$d_{ij} = \left\| x_j - v_i \right\| \tag{3.8}$$

3. Where, $X=\{x_1, x_2, \ldots x_n\}$, is input data points.Compute matrix U corresponds to classification of given points with the binary membership value of j^{th} point to i^{th} cluster in such a way that $U=[u_{ij}]$ where $u_{ij} \in \{0,1\}$ for all i and j:

$$\left\{ \begin{array}{ll} \sum_{j=1}^{k} u_{ij} = 1; & for\ all\ \ j \\ 0 < \sum_{j=1}^{n} u_{ij} < n\ ; & for\ all\ \ j \end{array} \right\} \tag{3.9}$$

4. Resuming calculation of cluster centers by averaging all pixels in cluster.

$$v_i = \frac{\sum_{j=1}^{n} u_{ij} x_j}{\sum_{j=1}^{n} u_{ij}}\ ; \quad for\ all\ i \tag{3.10}$$

5. If a cluster mean is the same with previous iteration, stop otherwise go to step.

Actually K-Means attempts to find one mean in each cluster. It defines means by picking K samples randomly and then follows the two iterations. It assigns each point to nearest mean and substantially moves mean to center of its clusters. The process easily can be seen in Figure 3.4, there are two clusters defining by red and blue colors and for each cluster you can see corresponding centers.

This algorithm aims at minimizing an objective function, e.g. a squared error function. The objective function $J(U,V)$ is:

$$J(U,V) = \sum_{i=1}^{k} \sum_{j=1}^{n} \left\| x_j - v_i \right\|^2 \tag{3.11}$$

Where $\|x_j - v_i\|$ is a chosen distance measure between a x_j data point and the cluster center, v_i, is an indicator of the distance of the n data points from their respective

cluster centers. Figure 3.4 shows sample lena image segmented by k-means is shown as follows:

Figure 3. 4: a) Lena image, b) Segmented image using K-Means

To undestand better there is a block diagram in Figure 3.5, which indicates the K-Means process as well.

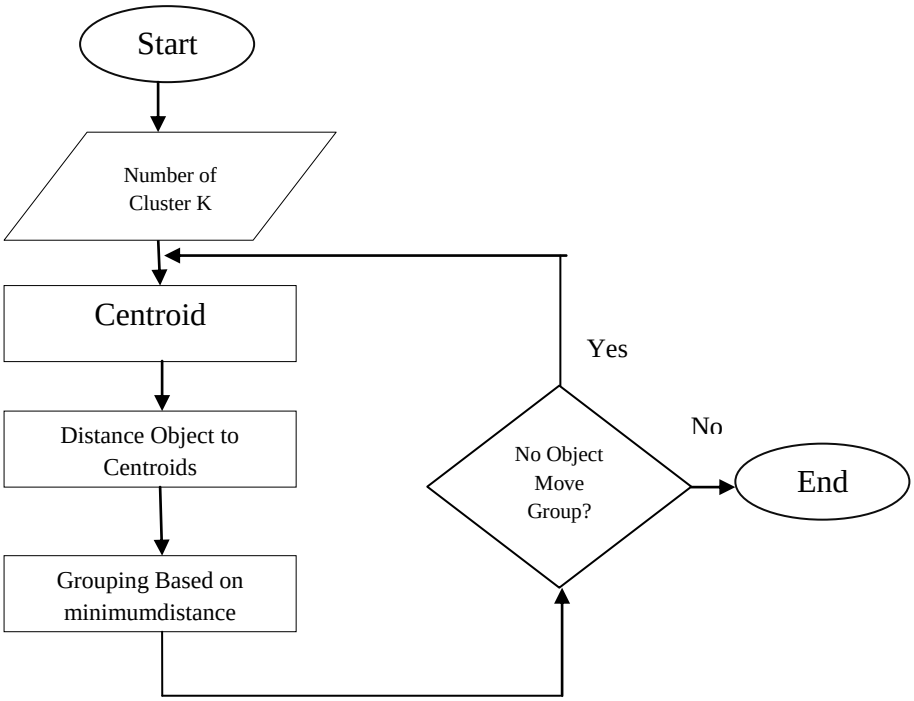

Figure 3. 5: Block Diagram of K-Means Process

1. Place K points into the space represented by the objects that are being clustered. These points represent initial group centroids.
2. Assign each object to the group that has the closest centroid.
3. When all objects have been assigned, recalculate the positions of the K centroids.
4. Repeat Steps 2 and 3 until the centroids no longer move. This produces a separation of the objects into groups from which the metric to be minimized can be calculated.

Figure 3.6 is an illustration of K-Means algorithm. First we choose two cluster centers shown in red color, then the algorithm assign each obects to centers which is most similarto them. In next step K-Means updates the cluster means then reassign objects to most similar centers again and this step is repeated until the centroids do not move anymore.

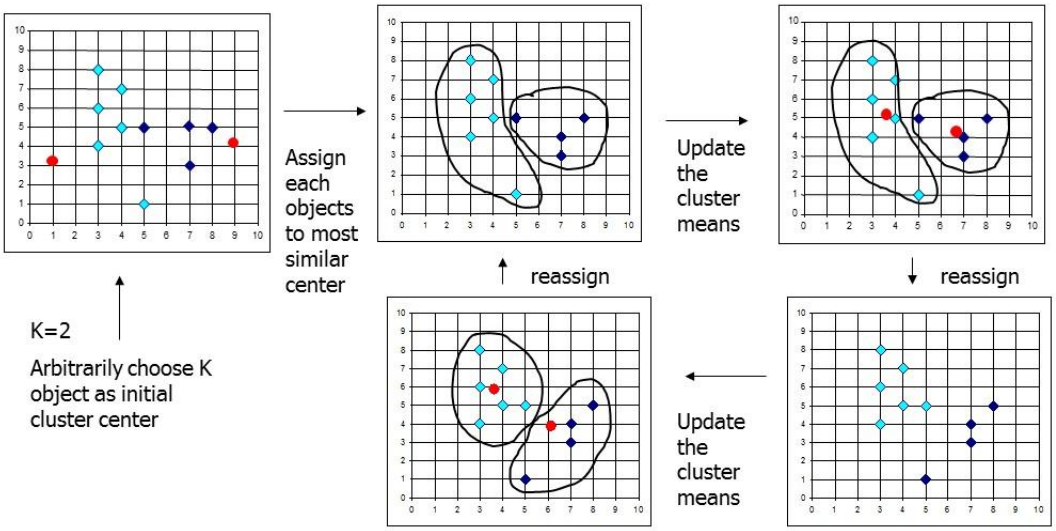

Figure 3. 6: Typical K-Means Algorithm [30]

Chapter 4

FUZZY C-MEANS CLUSTERING

As an unsupervised technique, Fuzzy clustering [31] has been successfully hired by feature analysis, clustering, and classifier designs in different fields such as astronomy, geology, medical imaging, target recognition, and image segmentation. Had been proposed by Bezdek in 1981 [32] Fuzzy C-Means clustering is one of the prominent fuzzy clustering algorithms applied in image segmentation. FCM is a soft clustering algorithm, which can efficiently overcome the segmentation problem.

Recently Fuzzy segmentation has become a widely used segmentation in medical imaging process mainly in analysis of anatomical structures. Unlike hard segmentation, this soft type of segmentation has an appropriate competency to exempt out more details and information from an input image. In fuzzy algorithm each data points can belong to more than one cluster and then assign each data points to a set of membership levels. These levels signify the strength of relationship among defined data elements and its specific cluster. It can classify the data (pixel) into defined number of clusters according to fuzzy membership scale, which is concluded by measure of membership.

The fuzzy membership scale is limited random number between zero and one, indicates the degree of similarity between the pixel value at that point and prototypical pixel value called, centroid, of pixel class. When a membership value

approaches to unity, consequently the degree of similarity between pixel and centroid in that specific cluster would be considerably high.

In another word FCM partitions the definite number of n points into c clusters with respect to some predefined features. Given the finite number of data points the FCM algorithm refrain a list of clusters and a partition matrix. Since the result critically relies on number of clusters, the method requires an initial definition of number of clusters. Like a K-Means algorithm Fuzzy C-Means attempts to reduce the objective function or cost function.

Actually FCM clustering can be achieved by iteratively decreasing a cost function that is related to the distance of the pixels to the cluster centers in feature space. Since pixels in an original image are highly correlated, the immediate neighborhood pixels present approximately the same attribute data. Subsequently, the spatial relationship of neighboring pixels is a main feature which can be considered an efficient aid to segment images [33] The fuzzy clustering algorithm is an iterative clustering method which can produces an optimal *c* partition by minimizing the weighted within group sum of squared error objective function *J* [34]:

$$J_m = \sum_{i=1}^{N}\sum_{j=1}^{C} u_{ij}^{m} \left\| x_i - c_j \right\|^2 A \quad , \qquad 1 \le m < \infty \tag{4.1}$$

Where *u* is a fuzzy *c*-partition of $\boldsymbol{X}$, *c* stands for vectors of centers, u_{ij}^{m} is the degree of membership of x_i in the i^{th} cluster, $\boldsymbol{X} = \{x_1, x_2, ..., x_k\}$ is data set in *N*-dimension vector space, *N* is the number of initial data, *C* is the number of clusters in $\boldsymbol{X}$ with limit $2 \le C <$ n, m is a weighting exponent on each fuzzy membership, c_j implies the center of cluster i, $c_i = \{c_{i1}, c_{i2}, \ldots c_{in}\}$, $\| \ \|_A$ is an induced *A*-norm on (n-dimension),

A is a positive definite $n \times n$ matrix , $\|x_i - c_j\|$ illustrates the distance between object and cluster center.

The Fuzzy partition can be derived within an iterative optimization of objective function shown in equation (4.2):

$$u_{ij}^m = \frac{1}{\sum_{k=1}^{C} \left(\frac{\|x_i - c_j\|}{\|x_i - c_k\|} \right)^{\frac{2}{m-1}}} \quad , \quad c_j = \frac{\sum_{i=1}^{N} u_{ij}^m \cdot x_i}{\sum_{i=1}^{N} u_{ij}^m} \tag{4.2}$$

Where, u_{ij}, is a membership of objective function. The iteration stops when $\max_{ij} \left\{ \left| u_{ij}^{(k+1)} - u_{ij}^{(K)} \right| \right\} < \varepsilon$ while ε represents a limitation criterion between 0 and 1 and *k* is the iteration step.

The distance between x_i and c_j given in equation (4.1) can be computed in this way:

$$d_{ik}^2 = \|x_i - c_j\| = (x_i - c_j)^T (x_i - c_j) \tag{4.3}$$

Where, T shows the transition function. In this formula the added weight u_{ij}^m betrays the m^{th} power of x_i membership within i^{th} cluster. Among all variables shown in equation (4.1) two of them hold an important role in J_m which needs to be pondered carefully, these two are *m* and *A*. The weighting exponent m manipulates the relative weights placed on each error. Increasing in m values subsequently could decrease the membership toward the fuzziest mood. There is not any document which could give the optimal value of m. The values in this range $1.5 \le m \le 3$ may give good results in most data sets.The second parameter which deserves extra respect is *A*. *A* is a weight

matrix can judge the final shape of optimal cluster in R^n. Any norm on n-dimensional *R* space can be computed by means of an inner product function as follows:

$$\langle X,Y\rangle_A = X^T AY \tag{4.4}$$

Although many kinds of *A*-norms are accessible to obtain in equation (4.1), practically few of them show the best performance. In FCM algorithm there are three choices to be applied, equation (4.1) will clearly shows these choices:

$$\begin{cases} A = I \rightarrow Euclidean Norm \\ A = D_x^{-1} \rightarrow Diagonal Norm \\ A = C_x^{-1} \rightarrow Mahalonobis Norm \end{cases} \tag{4.5}$$

More details of these different norm choices can be referred in Bezdek (1981) [35]. When *A* is identity matrix, *J* has produces hyper spherical clusters. When the choice is diagonal norm, each dimension is measured by its Eigen values.when extensive experiment used geological data, the only choice is to apply Euclidean norm in equation (4.1). An optimal solution of the object function *J* can be reached via chronological steps within Fuzzy C-Means algorithm as [32]:

1. Define the initial values of *c*, *m* and *A*.
2. Choose the initial fuzzy partition matrix $U = [u_{ij}]$ with $j = \{0,1,\ldots,L\max\}$
3. Compute $C = [c_j]$ varying $i, i = \{1,2,...,c\}$:

$$c_j = \frac{\sum_{i=1}^{N} u_{ij}^m \cdot x_i}{\sum_{i=1}^{N} u_{ij}^m}; \quad 1 \le j \le C \tag{4.6}$$

4. Calculate the membership matrix $U^{(k)}$,$U^{(k+1)}$ by:

$$u_{ij} = \frac{1}{\sum_{k=1}^{C}\left(\frac{\|x_i - c_j\|}{\|x_i - c_k\|}\right)^{\frac{2}{m-1}}} \quad ; \quad 1 \le k \le N,\ 1 \le i \le C \tag{4.7}$$

5. Compare $U^{(k+1)}$ and $U^{(k)}$ in optimal matrix norm. If, $\|U^{(k+1)} - U^{(k)}\| < \varepsilon$ stops otherwise, set $U^{(k+1)} = U^{(k)}$ and go back to step 3.

To better understanding, there is a simple example of a mono-dimensional application for FCM segmentation algorithm [36]. In this example twenty data points are used and the cluster number is 3. Figure 4.1, illustrates the membership values for each point in each cluster. Each color shows the nearest cluster with respect to the membership.

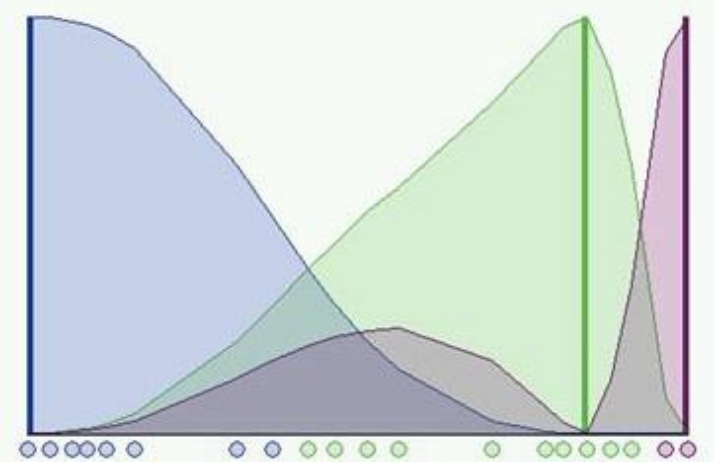

Figure 4. 1: A Sample of FCM for Twenty Data and three Clusters [36]

In Figure 4.2 the fuzziness coefficient is *m*=2 when $\max_{ij}\left\{u_{ij}^{(k+1)} - u_{ij}^{(k)}\right\} < 0.3$ is the termination is considered for algorithm. You can see the initial condition in which fuzzy distribution relis on exact position of each cluster. This figure shows the final output reached at 8th step of FCM performance with *m*=2 and $\varepsilon = 0.3$.

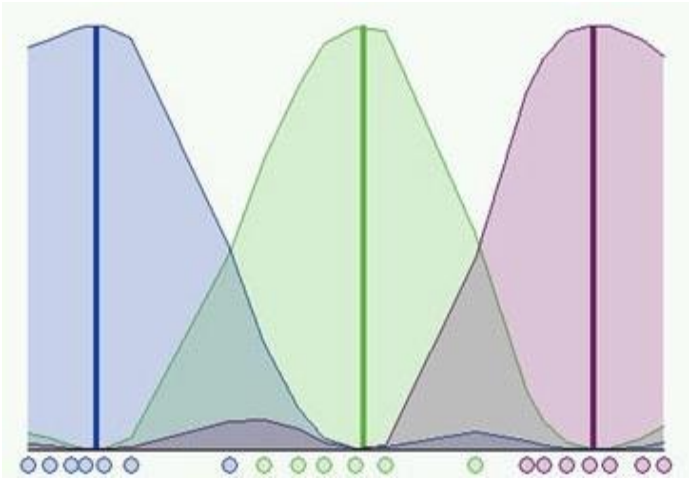

Figure 4. 2: FCM Result of segmentation with *m*=2 & $\varepsilon = 0.3$in 8^{th} step[36]

In order to have higher accuracy we increase the steps of FCM segmentation process and Figure 4.3 is result of same data is achieved in high itrations.

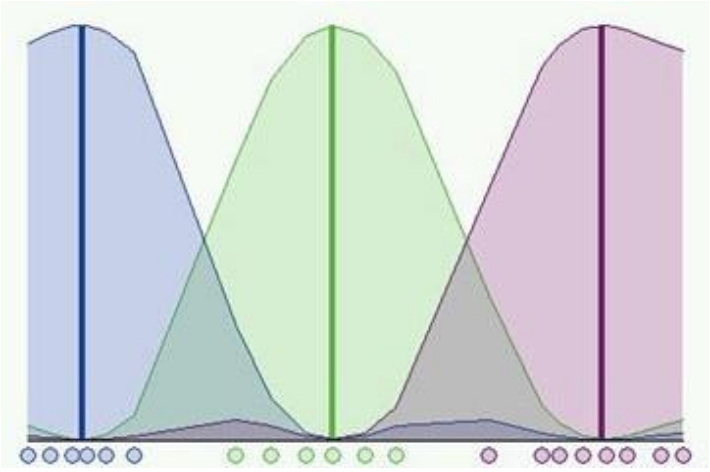

Figure 4. 3: FCM Result of segmentation with *m*=2 & $\varepsilon = 0.01$in 37^{th} step[36]

Chapter 5

PSEUDO-COLORING

A Magnetic resonance image is a kind of multi-modality image, which requires multi-dimensional feature space often is shown in eight or higher bits gray scale. Though, it is not yet proved that the higher gray scale resolution may communicate more information of a MR image. The experimental results indicate that the well-designed pseudo-color MR images will display enhanced performance particularly in precise detection of lesion region in brain images. The pseudo-color method which is used in this work is CIE L*a*b* uniform method. The method employs HSI space to convert a gray scale image to color image.

5.1 HSI Color Model

This model consists of three important coefficients called Hue, Saturation and Intensity. Hue factors displays purity of colors in Red, Green and Blue for instance pure Green. Saturation represents a degree in where Hue is attenuated by white light. Finally Intensity shows the gray scale levels of each color. Two coefficients H and S carry the chrominance or color information of an image, which is very close to a perspective method in human vision, while I coefficient includes only luminance or gray scale information of image. These advantages lead mentioned space to adapt easily to human vision efficiently. To indicate clearly, a standard HSI model is shown in figure 5.1:

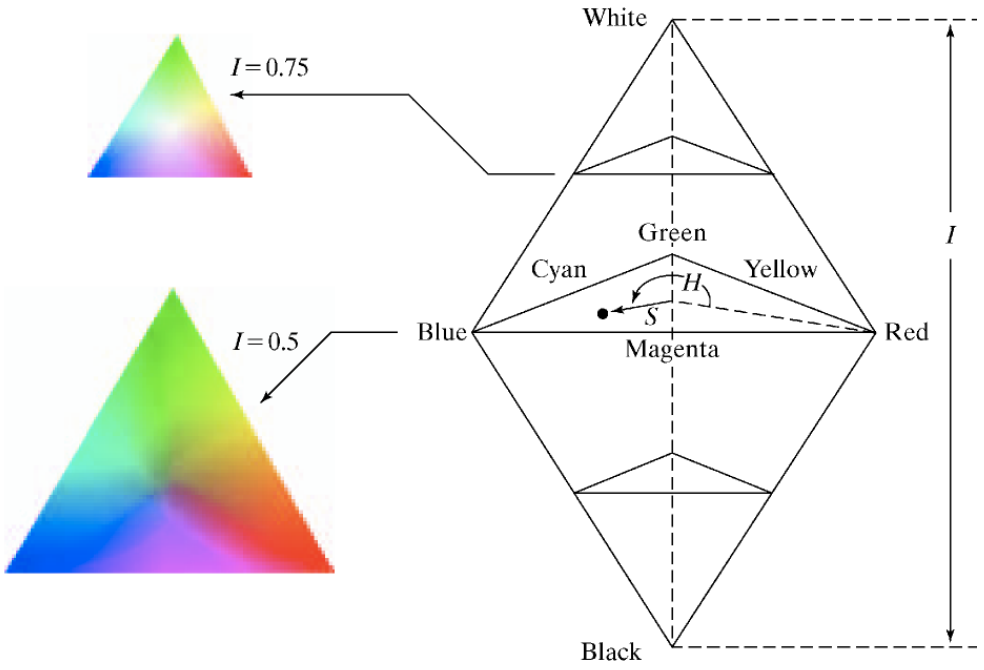

Figure 5. 1: A standard HSI space model [37]

As the figure shows the intensity ranges starts from 0 (black) to 1(white). The Hue factor is varying between 0 to 2π .The lowest value for saturation range is 0 while the maximum possible point for saturation is 1.

5.2 Transform a Gray-Scale Image to HSI

An 8-bit gray scale MR image gray level of pixels is shown by $g(x, y)$where $0 < h(x, y) < 255$ is hue component of image [38], [39]. The method is as follows:

$$h(x,y) = 255g(x,y)/\max g(x,y) \tag{5.1}$$

$$H = 2\pi h(x, y)/255 \tag{5.2}$$

$$I = h(x,y) \tag{5.3}$$

$$S = \begin{cases} kh(x,y) & h(x,y) \le 127 \\ k(255 - h(x,y)) & h(x,y) > 127 \end{cases} \tag{5.4}$$

Here, there is a considerable direct relationship among *k* and saturation factor subsequently the range of saturation can be varied between 0 and 255 by changing *k* coefficient from 0 to 2. In this thesis the chosen amount for *k* is 2. After reaching out to *I*, *H* and *S* components (three basic factors in HSI space) next aim is to transform pseudo-color image to RGB space.

5.2 HSI to RGB Transformation

RGB is a kind of space in which all colors can be seen in their own primary color spectral components of Red, Green and Blue. The following model simply describes the RGB model in 3 dimensions Cartesian coordinate system.

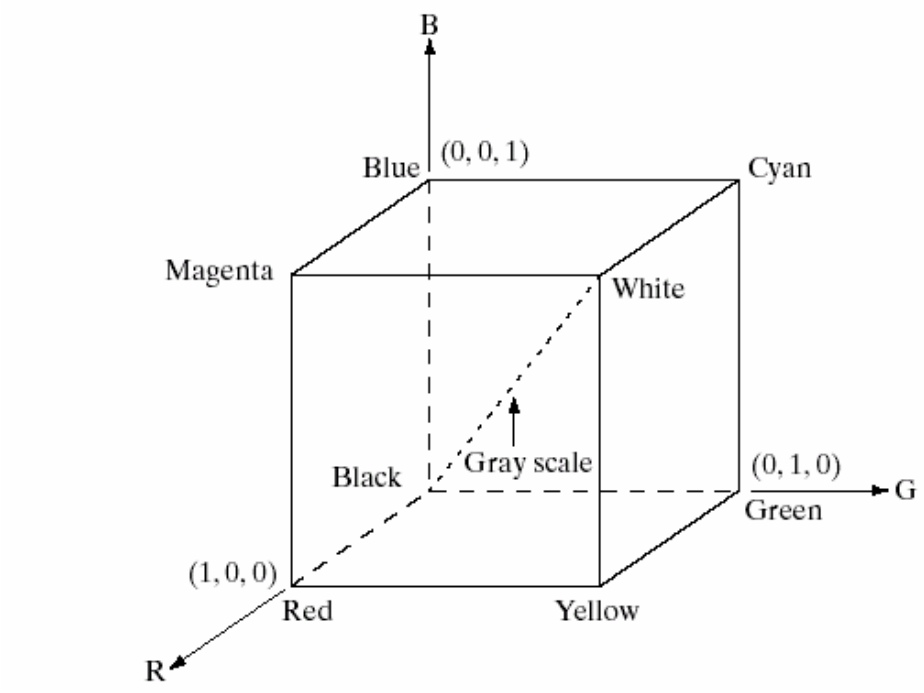

Figure 5. 2: RGB in 3D Cartesian cordinate system [40]

Note that, the coordinate (0, 0, 0) represents black and (1, 1, 1) represents white. To reach a RGB image all R, G and B components of an image should have been combined .the process of RGB image is shown here:

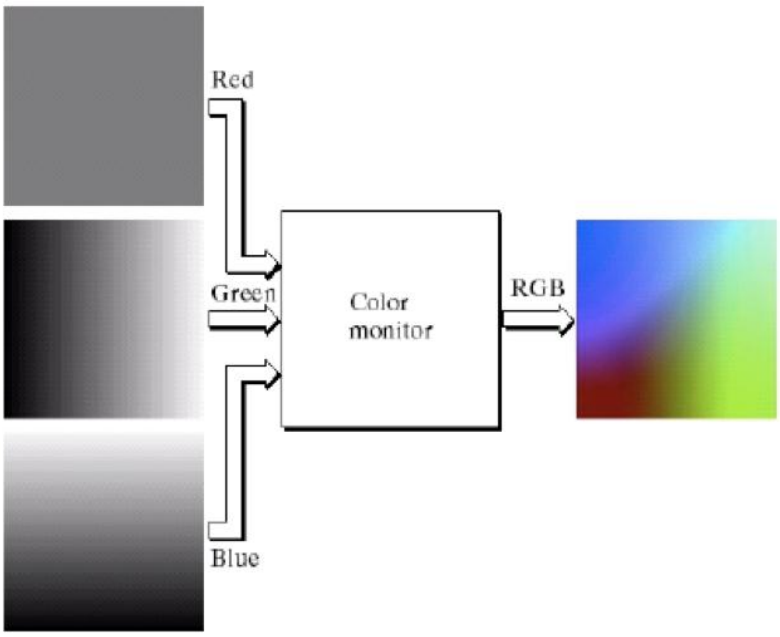

Figure 5. 3: Formation of RGB Image [40]

RGB components can be computed via this equation gently [41]:

$$\begin{cases} V_G = S \bullet \cos(H) \\ V_R = S \bullet \sin(H) \end{cases} \tag{5.5}$$

$$\begin{pmatrix} R \\ G \\ B \end{pmatrix} = \begin{pmatrix} 1 & -0.204124 & 0.612372 \\ 1 & -0.204124 & -0.612372 \\ 1 & 0.408248 & 0 \end{pmatrix} \begin{pmatrix} I \\ V_G \\ V_R \end{pmatrix} \tag{5.6}$$

5.3 RGB to La*b* Transformation

The CIELab is a kind of perspective uniform color difference system adopted by CIE stands for commission International de I'eclairage in 1976. The CIELab is a based on color difference equation implemented by E.Q Adams and D.Nickerson in early 19's

to scale color fading in textile industry. As an appropriate choice the system attempts to utilize xyz coordinates to assess reliable information of a color image. Actually it leads to compute color difference scores. The system has three channel, one luminance channel namely L and two chrominance channels a* and b*. The CIE La*b* model is at follows:

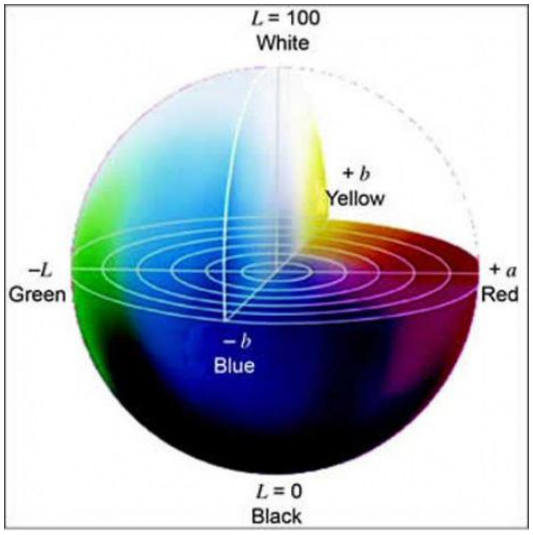

Figure 5. 4: A CIE La*b* color space model

The first step is to find chromatics that is defined in [42]:

$$\Delta E = ((\Delta L)^2 + (\Delta a^*)^2 + (\Delta b^*)^2)^{\frac{1}{2}} \tag{5.7}$$

The initial values are:

$$Initial\ Values = \begin{Bmatrix} x_0 = 94.852 \\ y_0 = 100 \\ z_0 = 107.381 \end{Bmatrix} \tag{5.8}$$

The following equations represent the relation between RGB and CIELa*b* spaces.

$$g(x) = \begin{Bmatrix} x^{0.53} & x > 0.008856 \\ 7.787x + 0.137931 & x \le 0.008856 \end{Bmatrix} \tag{5.9}$$

$$\begin{pmatrix} x \\ y \\ z \end{pmatrix} = \begin{pmatrix} 0.43395 & 0.37622 & 0.18983 \\ 0.21267 & 0.71516 & 0.07217 \\ 0.01776 & 0.10984 & 0.87276 \end{pmatrix} \begin{pmatrix} R \\ G \\ B \end{pmatrix} \tag{5.10}$$

$$Transformation\ \ Equations = \begin{cases} X = g\left(\dfrac{x}{x_0}\right) \\ Y = g\left(\dfrac{y}{y_0}\right) \\ Z = g\left(\dfrac{z}{z_0}\right) \end{cases} \tag{5.11}$$

And finally *L*, *a**, and *b** component of La*b* color space derived by using equation 5.12 in this way:

$$\begin{cases} L = 116Y - 16 \\ a^* = 500(X - Y) \\ b^* = 200(Y - Z) \end{cases} \tag{5.12}$$

Chapter 6

PROPOSED CLUSTERING BASED SEGMENTATION METHODS

6.1 Introduction

In order to segment the MRI T1w images, it is crucial to use multi dimensional segmentation algorithm, which uses multiple parameters of interests. So, medical images could easily be classified into different numbers of classes through pixel classification by this way. The number of classes corresponds number of clusters of an input image. The segmentation algorithm is probing the neighborhood pixels according their labels, looking for same class label to make a new region of interest whole along the segmentation process. However, segmentation algorithm can choose the wrong region of input image, which is out of region of interest and may report useless information of image. We apply a simple brain mask, as a post processing technique to extract unwanted regions leads to obtain truly final segmented output. Following Segmentation process indicates how to utilize a color-converted segmentation algorithm based on K-Means and Fuzzy C-Means clustering in order to detect and extract tumor region in brain.

6.2 Transform Input RGB Image to La*b*

The first step is to transform input Gray-scale image to HSI color space. The next step is to find HSI components: H, S and I. H refers to hue component of image, S

refers to saturation and I refers to intensity parameter of image. To convert HSI Image to RGB space, Red, Green and Blue, next step is to convert imege in RGB space to La*b* color space, which consists of luminosity layer L and two chromaticity layers, a* and b*. a*, shows the place where color falls into red-green axis and b* shows the place where color falls to blue-yellow axis in standard color space. To show the overall process in a short view, the block diagram is shown in Figure 6.1:

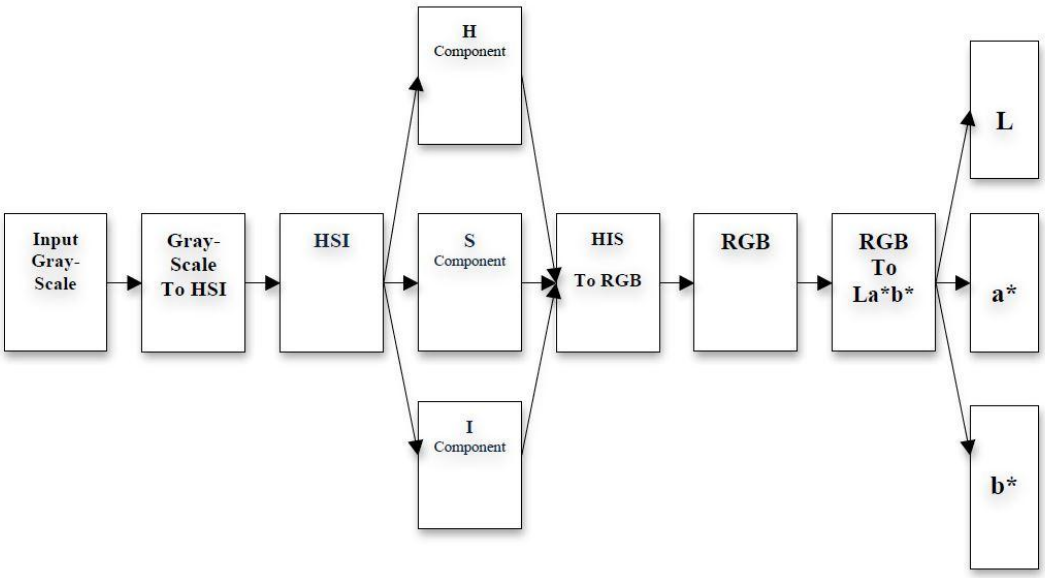

Figure 6. 1: Block Diagram of Pseudo-Coloring

6.3 Applying K-Means Algorithm

Since a* and b* layers contain all the color information of image they are used to segment the image pixels. The difference between two layers can be computed by segmentation algorithm. We apply a* and b* components to test algorithm, K-Means. First we apply the calculated a* and b* components of input image to K-Means, difference between two layers in this technique be computed by means of Euclidean metric. The pixels of image be segmented to n clusters, each cluster gives different segmented images among theses images we choose the result image which contains the region of interest, tumor region of input brain MRI T1w image in the

final output. The last step is a post-processing step, applying a brain mask to chosen segmented cluster to erode unwanted regions and get the segmented tumor region. After all, to show the tumor region clearly, we use a morphological dilation operation on tumor region and the outcome is a segmented tumor with green edge contour around it. The visual results of process, is available in next chapter. The summary of k-means segmentation process can be seen in Figure 6.2:

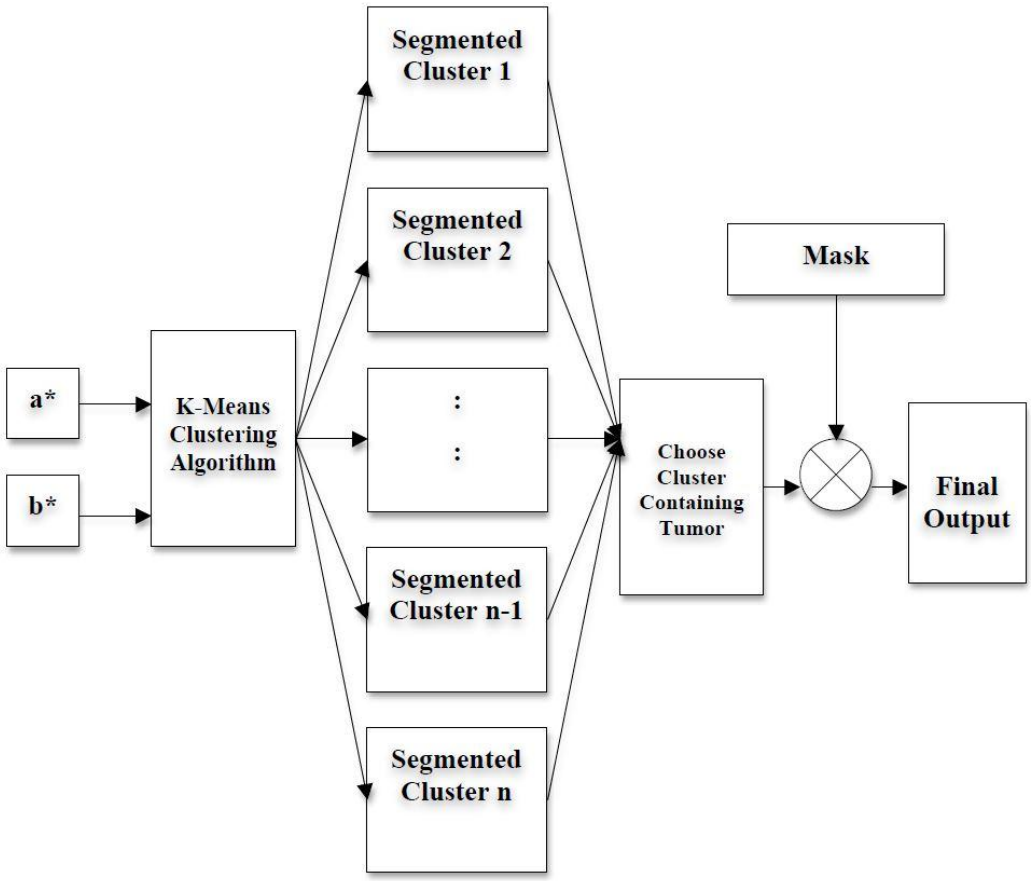

Figure 6. 2: Block Diagram of K-Means Segmentation Process

6.4 Applying Fuzzy C-Means Algorithm

In this step we apply the proposed segmentation method to a* and b* components in order to segment the given image. The difference between two layers can be calculated through FCM method. FCM method, gives n clusters of given image and

in this time the best result, which is showing tumor region clearly, is chosen manually. Like the previous algorithm, a simple brain mask is applied to segmented image to get rid of unwanted region around brain like brain skull or skin. Again we add a green edge contour to tumor region to display the region obviously. The segmented result of given test image can be found in next chapter which contains our experimental results. The process of proposed segmentation algorithm shown in figure 6.3:

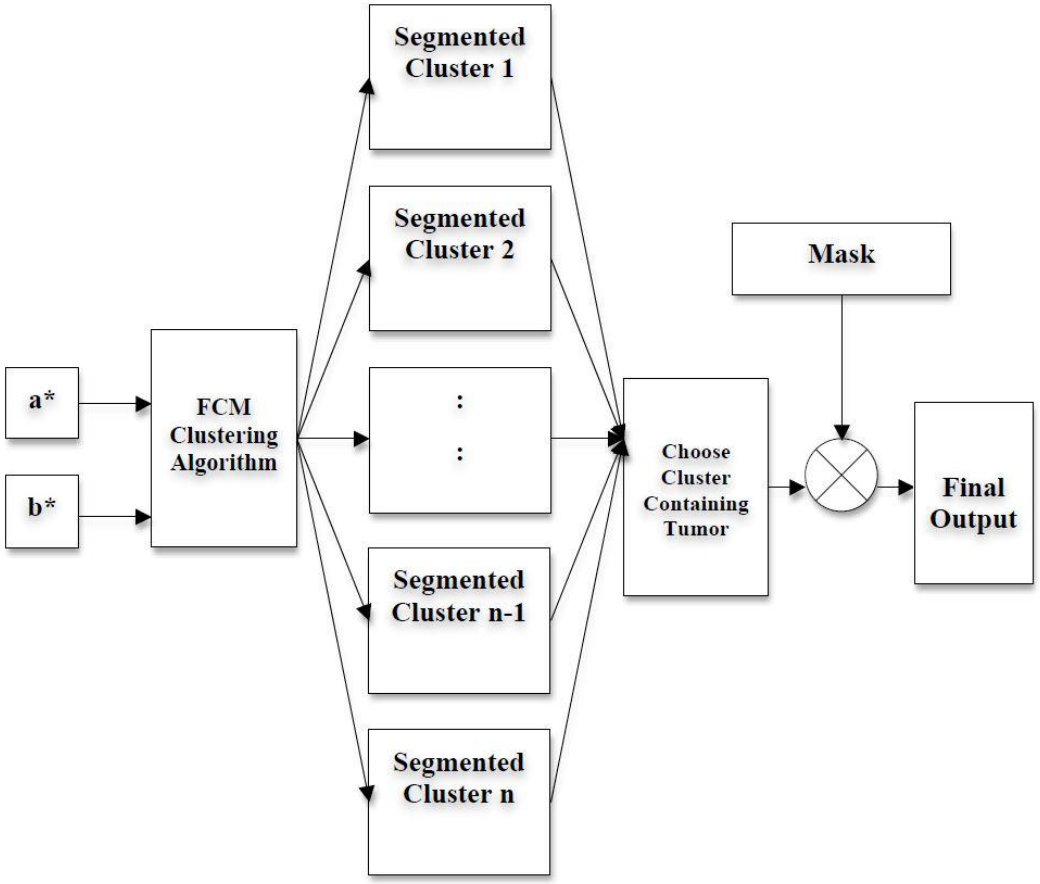

Figure 6. 3: Block Diagram of Fuzzy C-Means Segmentation Process

6.5 Post-Processing

The aim of segmentation process is to diagnose the lesion region tumor or edema so to cover this, after clustering process the non important parts of brain namely are skin, skull and fat are eliminated and the rest is our region of interest for

segmentation including just lesion regions. Subsequently the final output could clearly give the tumor region of patient brain. This process is shown in both Figure 6.2 and Figure 6.3 as a mask block which is multiply to chosen segmented cluster before reaching to final output.

Chapter 7

EXPERIMENTAL RESULTS & ANALYSIS

7.1 Introduction

MRI images are absolutely the best choices in medical imaging methods to evaluate the performance of segmentation method particularly when soft tissue is required. In this thesis, we propose a new approach for detecting lesion in brain based on pseudo-colored FCM method, which attempts to distinguish the lesion region from other healthy tissues in brain. Brain MRI has three slice maps called transverse, coronal and Sagittal in 3 directions of a head [43]. The transverse slice map consists of three types of images namely are T1weigthed, T2weigthed and PD weighted images. T1 and T2 modes are multispectral while PD is single channel. The multi-spectral images are capable to provide sufficient information of anatomical tissues rather than the single channel mode. T1 and T2 weighted images refer to several scans, which investigate the fluctuation of spinlattice or relaxation time of various tissues in vessels. The pathologist injects a kind of fluid in vessels, as a consequence it makes a variation in some tissues then they calculate the time, which takes to retain to their initial moods. This period of time leads to come out T1 and T2 MRI images. Although both types have some characteristics in common, they carry small dissimilar features. In T1 images fat is white and Fluid and water are black while in T2 images fat is dark and rest are bright. T1 images have high contrast and low noise and also long relaxation time in comparison with T2 images. So we apply

T1weigthed (multi-spectral) brain MRI images to test our proposed method. In order to measure the performance of new segmentation method generally it is required to have pathological ground truth, which exhibits the real tumor of a patient in clinical MRI tests.

In this thesis the Brain Web dataset, which contains multi-modal MR images of normal brain structures, applied as the healthy brain pathological ground truth. Next step is to have synthetic tumor images in which the deformation in brain caused not only by chemical changing in brain but also designed by a software called 3D slicer, which can implant any kind of tumor on a healthy brain image [44] . Finally we generated our own synthetic MRI brain images with lesion region to measure the validation of our proposed segmentation method.

7.1.1 Original T1w Images

Actually the process of evaluation requires one original set of MR images with lesion regions taken from real patient cases observed in clinical dataset, which could obviously illustrate true size and location of real lesion including tumor or edema.The original set of T1w MR images, ten real images, is shown in Figure 7.1 a-j. As you can all of them are taken from real patients with deformation mass in one part of their brains. In all real images tumor region is clearly can be seen in bright color among the brain skull. Actually the lesion region refers both tumor and/or edema regions in brain image.

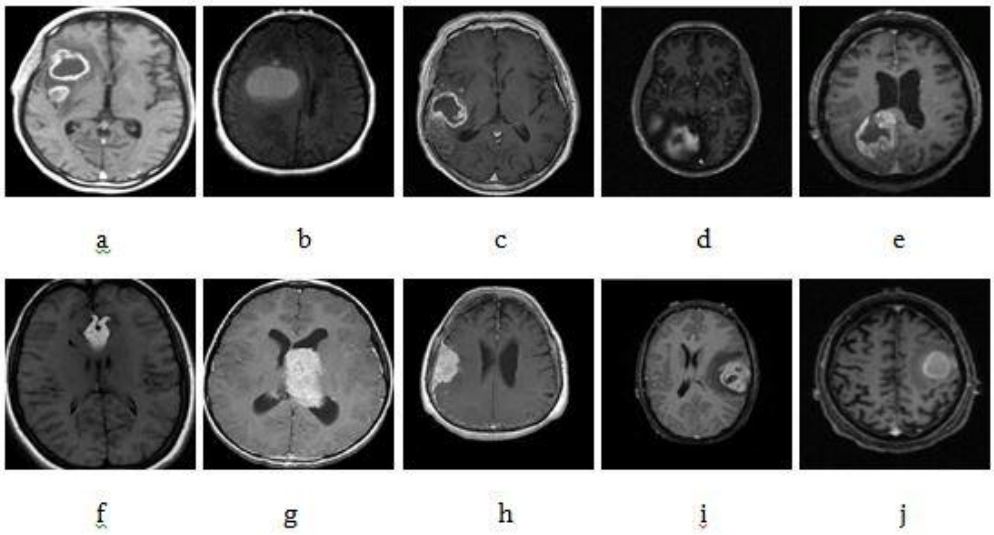

Figure 7. 1: a-j) Real T1w Brain MRI Images with Tumor or Edema [45]

7.1.2 Synthetic Set Of MR Images

In order to have a precise and reliable validation of our proposed method it is also appropriate to have a synthetic brain images with lesion criterion. Subsequently two sets of synthetic T1 MRI images are obtained in this work. One synthetic enhanced T1w images, is generated by using a sort of medical application software called 3d slicer, that is thoroughly explained in and the other source, brain web synthetic data set. The synthetic T1w data set can be seen in Figure7.2, a-j. Like the previous real data set each ten images holds a type of lesion tumor or edema in different positions of brain.

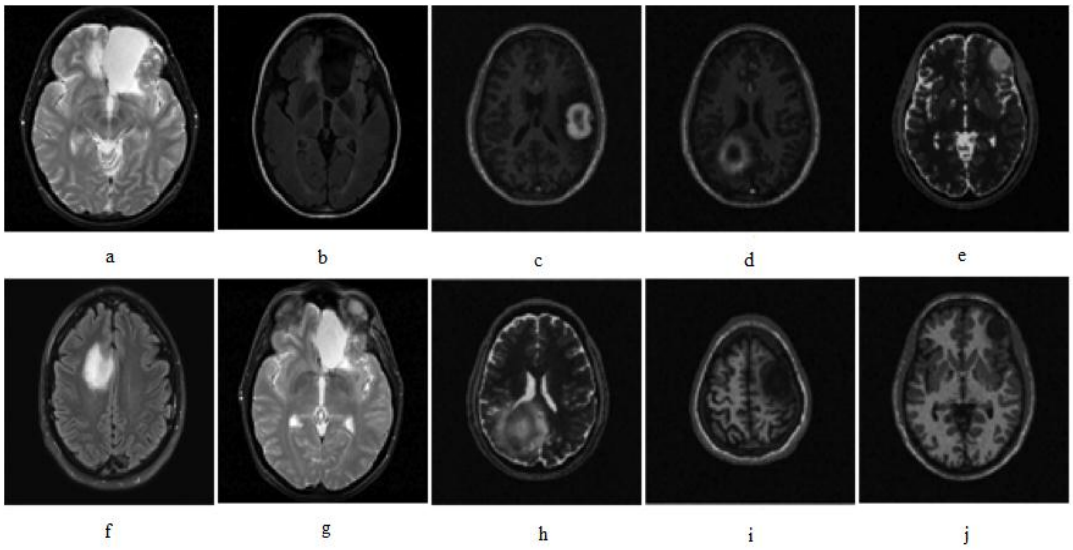

Figure 7. 2: a-j) Synthetic T1w Brain MRI Images with Tumor or Edema [46]

7.1.3 Generation of Synthetic T1w Data

The other synthetic set used in this experiment is our own generated synthetic set. To accomplish synthetic dataset, five healthy brain t1 images and five tumor masks have been chosen. The generation of our t1w synthetic images is clearly described and reached threw the block diagram shown in Figure7.3 . As the diagram illustrates, first a healthy T1w brain is chosen, then one tumor mask is multiplied to it. The outcome is a synthetic T1w brain image with a tumor in it.

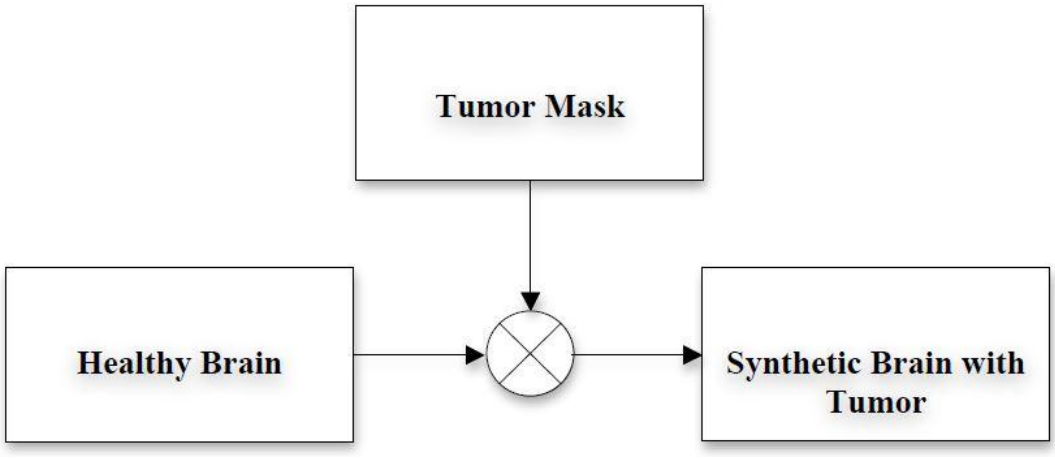

Figure 7. 3: Block Diagram of Synthetic Brain Image Generation with Tumor

As shown in Figure 7.4, we use five healthy T1w brain images in order to generate our synthetic data set. The chosen size of all images is 255×255 pixels and all of images are converted to gray-scale level.

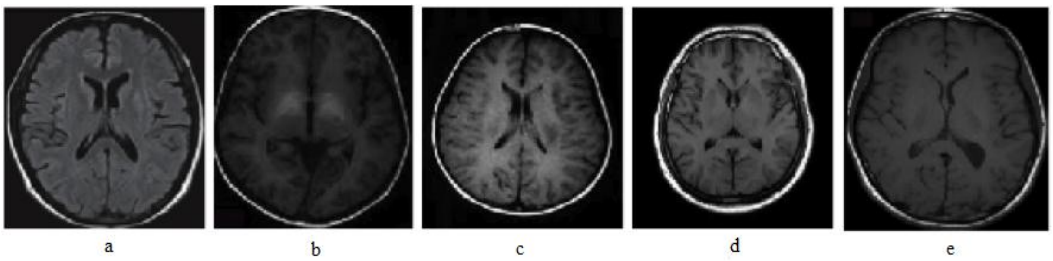

Figure 7. 4: Five Different Types of Healthy T1w Brain Images

The next step of synthetic data generation is to multiply real tumor mask to the used data set. Five real tumor masks have been presented in Figure 7.5. Again all of them are in same size 255×255 and in gray-scale level.

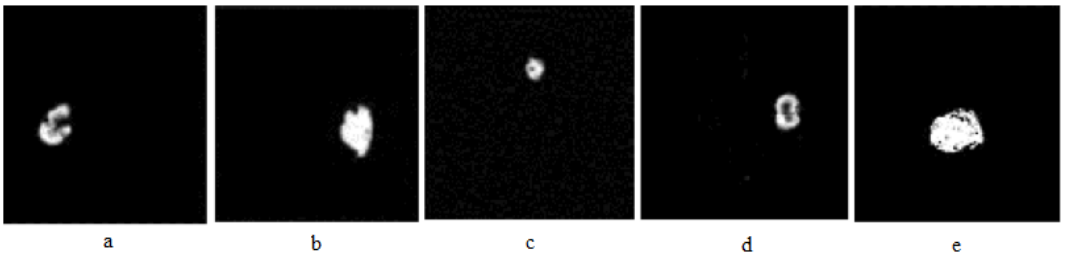

Figure 7. 5: Five Different Types of Tumor Masks

By multiply each five healthy dataset by five different tumor masks we get 25 different synthetic T1w brain images with five different types of tumors. The dataset is shown here in five groups each displays one type of tumor in five different brains. The groups are shown in Figure 7.6. As you can see, a-e images correspond to group 1, f-j images correspond to group 2, k-o images correspond to group 3, p-t correspond to group 4 and u-y images correspond to group 5 of our generated synthetic T1w brain dataset.

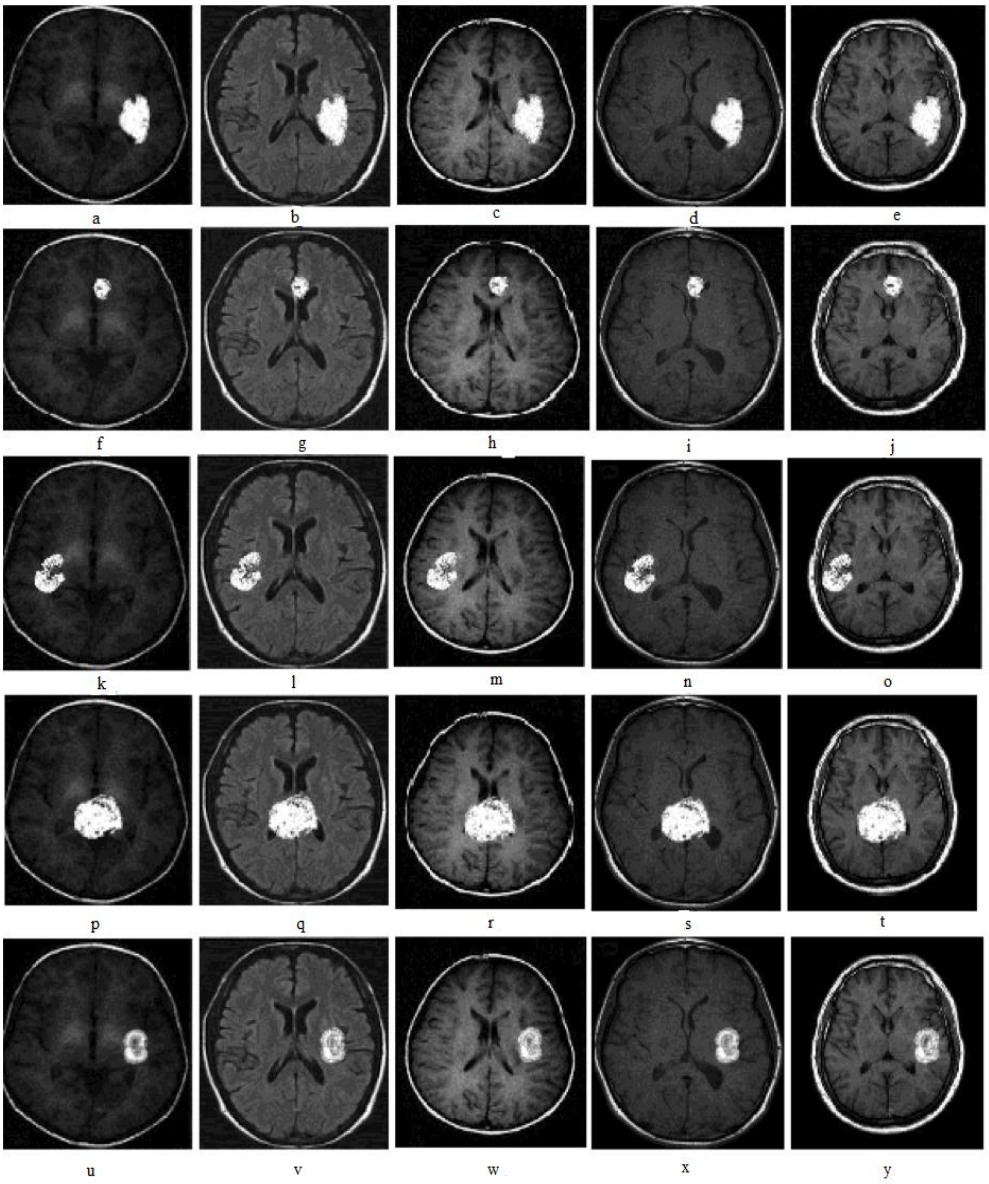

Figure 7. 6: Dataset Including Five Different Image Groups Generated by Five Different T1w Synthetic MRI Images and Tumor masks,a-e) Image Group 1, f-j) Image Group 2, k-o) Image Group 3, p-t) Image Group 4, u-y) Image Group 5

7.2 Experimental Methodology

7.2.1 Sensitivity & Precision

In order to evaluate the performance of proposed segmentation method and also investigate statistical results the true way is to compute sensitivity (or Recall) and precision for each test chain in image segmentation. Mentioned metrics could gently conclude a numerical report of overall experiments. Both metrics are common in

components namely are True positive, False positive, True negative and false negative [47]. Here the meaning of each term has been explained clearly:

- TP: Tissue pixel is correctly diagnosed as tissue pixel.
- FP: Non-tissue pixel incorrectly diagnosed as tissue pixel.
- TN: Non-tissue pixel correctly diagnosed as Non-tissue pixel.
- FN: Tissue pixel incorrectly identified as Non-tissue pixel.

After finding these parameters sensitivity and precision can be computed easily via these two equations:

$$sensitivity = \frac{TP}{(TP + FN)} \tag{7.1}$$

$$precision = \frac{TP}{(TP + FP)} \tag{7.2}$$

7.2.2 Segmentation Accuracy

To evaluate the performance of proposed method segmentation accuracy sounds to be a reliable and precise measurement approximately in all image segmentation algorithms. Segmentation accuracy can display the statistic results of a segmented image clearly which assist to have a fair comparison and judgment between one or more segmentation algorithms. The segmentation accuracy of an image can be computed via following formula [48]:

$$Segmentation\ Accuracy = \frac{(TP + TN)}{(TP + FN + TN + FP)} \tag{7.3}$$

7.2.3 Peak Signal to Noise Ratio (PSNR)

PSNR stands for Peak Signal to Noise Ratio is a widely used objective metric which can estimate the quality of a segmented image. By means of MSE or Mean Square Error this measurement can be employed to any processing system specially segmentation algorithms [49] . To have an exact validation the mentioned metrics require an original brain image to be referred as a ground truth. Given the ground truth image name *G* and test image *T* both images are $M \times N$ matrix, MSE between *G* and *T* can be defined as:

$$MSE(G,T) = \frac{1}{MN}\sum_{i=1}^{M}\sum_{j=1}^{N}(G_{ij} - T_{ij})^2 \tag{7.4}$$

PSNR between *G* and *T* can be reached by equation 6.2 by means of MSE parameter that gets from equation 6.2:

$$PSNR(G,T) = 10\log\left(\frac{255^2}{MSE(G,T)}\right) \tag{7.5}$$

The base of logarithm used in signal to noise ratio is 10.

7.2.4 Structural Similarity Index Measurement (SSIM)

Structural Similarity Index Measure or SSIM is a very popular evaluation metric, which measures the closeness between two given images in segmentation methods. Due to inform similarity degree of two images the approach would give out three different comparison functions namely are luminance comparison, contrast comparison and structure comparison. The general formula for SSIM can be seen in following [49]:

$$SSIM(G,T) = l(G,T)c(G,T)s(G,T) \tag{7.6}$$

The luminance comparison or can be computed in this way:

$$L(G,T) = \frac{2\mu_G \mu_T + c_1}{\mu_G^2 + \mu_T^2 + c_1} \tag{7.7}$$

Here, parameter represents the mean luminance of two images. The equation reaches its maximum value 1 when $\mu_G = \mu_T$ .The second comparison is contrast comparison in which,*C(G,T)* measures similarity of contrast between two images. It defined as:

$$C(G,T) = \frac{2\sigma_G \sigma_T + c_2}{\sigma_G^2 + \sigma_T^2 + c_2} \tag{7.8}$$

In this equation parameter signifies the standard deviations of two images. In the case that $\mu_G = \mu_T$ the term mentioned above meets its highest value at 1. The last comparison function is structure comparison function, which used to calculate the structure closeness between images *G* and *T*. The structure function is:

$$S(G,T) = \frac{\sigma_{GT} + c_3}{\sigma_G \sigma_T + c_3} \tag{7.9}$$

The parameters σ_G, σ_T, show the standard deviations of each images while parameter σ_{GT} signals the covariances between *G* and *T*.This term has a positive value until the SSIM indices take the values between 0 and 1. If the answer of equation is 0, it means there is no similarity between two images whereas the answer 1 informs the total correlation between them (*G=T*). The extra parameters C_1, C_2, C_3 are positive constants used to eliminate null denominator in above equations.

7.3 Pseudo Coloring Approach Results

In this section the steps of pseudo-coloring approach have been described by means of three arbitrary types of real brain T1 input images A, B and C with different tumor lesions. As mentioned in chapter 6, in first step the input brain T1 image has to be converted to gray-scale image. You can see three different converted real T1w brain images a, b, and c into gray-scale in Figure 7.7.

7.3.1 Gray scale image

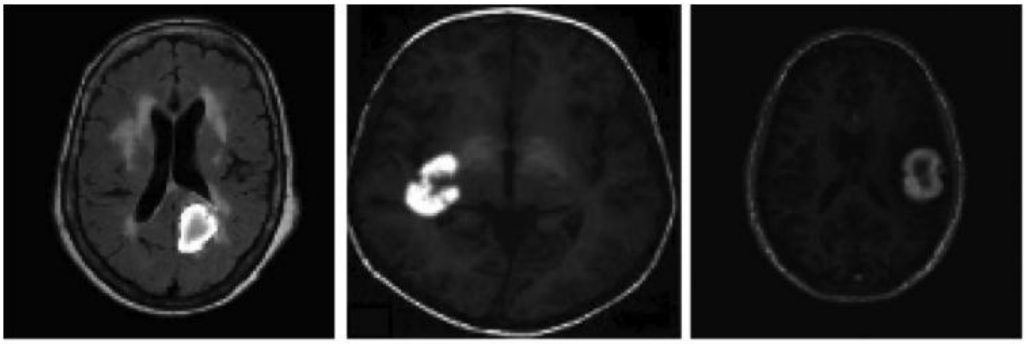

Figure 7. 7: a) Gray-Scale of Image A [38], b) Gray-Scale of Image B, c) Gray-Scale of Image C [7]

7.3.2 HSI Transformation

The second step is to transform grayscale images to HSI images the required equation for this transformation has mentioned in chapter 5 in details. The HSI result of three input images, are shown in following figures. In Figure 7.8 , a represents the H, hue component of given gray scale image, b shows the S or saturation component of given gray-scale image, c indicates the I component or intensity of given gray-scale image and d shows the input gray scale image, A in HSI space.

Formation of HSI of Image A:

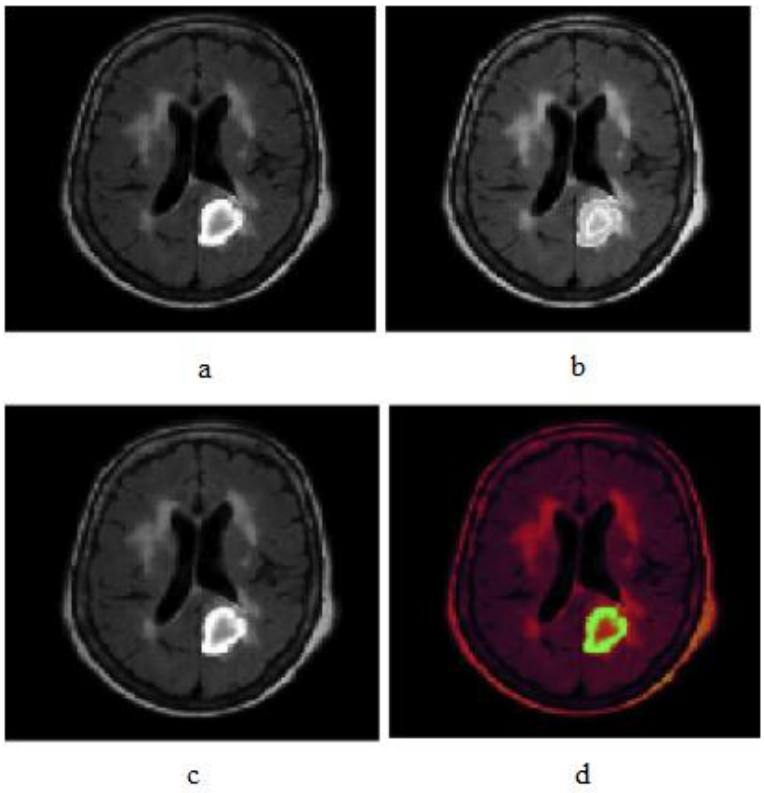

Figure 7. 8: a) H Component of A,b) S Component of A, c) I Component of A, d) Image A in HSI Space

Formation of HSI of Image B:

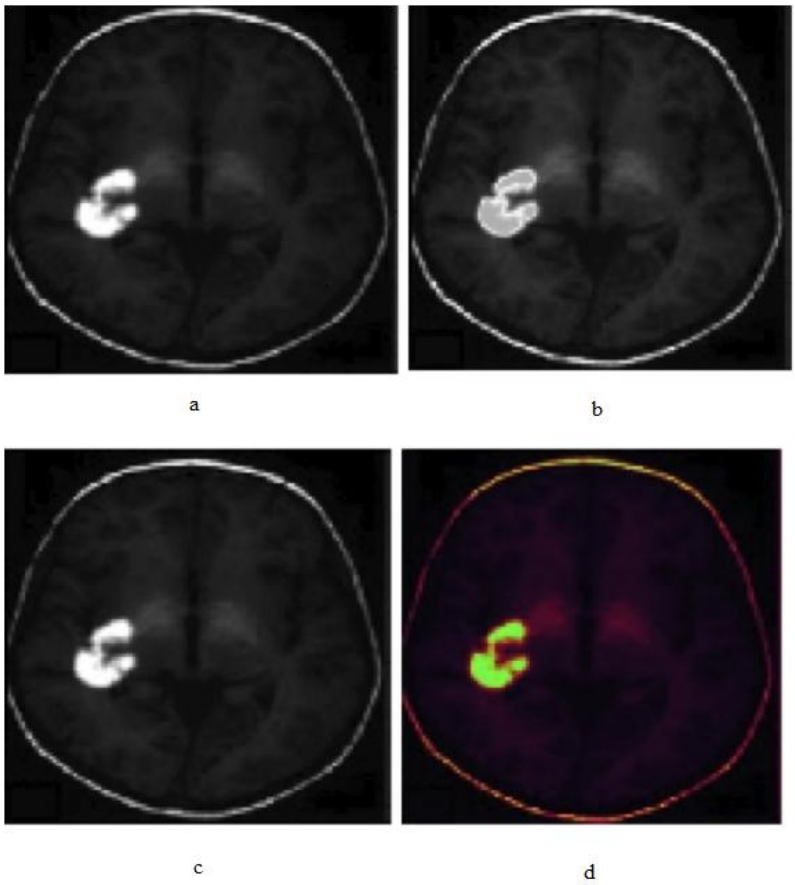

Figure 7. 9: a) H Component of B, b) S Component of B, c) I Component of C, d) Image B in HSI Space

In Figure 7.9, the transformation of HSI space of second test image B. In the Figure, a corresponds to H component or hue of second test image, b corresponds to S component or saturation of given test image, c corresponds to Intensity component or I of given test image, and at last d displays the given test image, in HSI color space.

Formation of HSI of Image C:

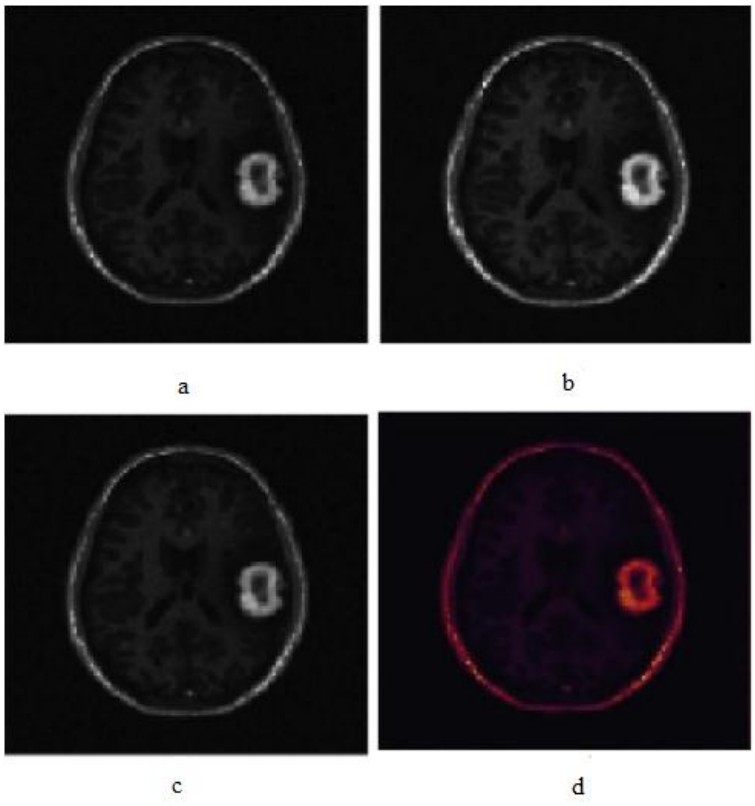

Figure 7. 10: a) H Component of C, b) S Component of C, c) I Component of C, d) Image C in HSI Space

Figure 7.10 contains HSI fromation of given test image C. Here, a shows the Hue component of image C,b shows the saturation component of image C,c shows the intensity component of given test image C and finally d illustrats the given test image C in HSI color space.

7.3.3 La*b* Transformation

In this section a*b* components of La*b* test images via CIELa*b* equation already defined in chapter 5. The input test results in La*b* color space can be seen here.

La*b* formation steps of Image A:

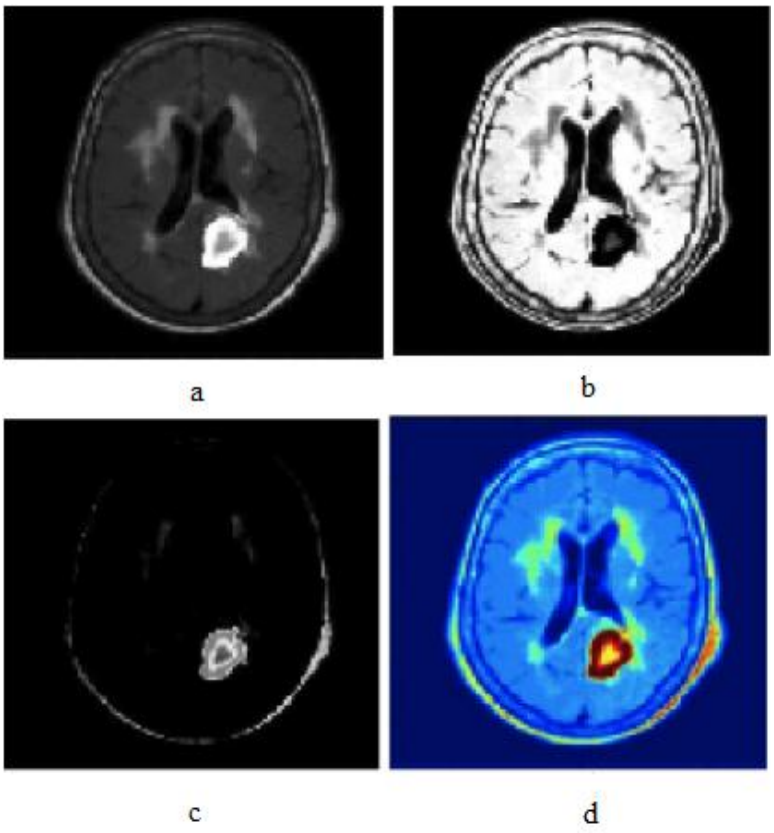

Figure 7. 11: a) L Component of A, b) a* Component of A, c) b* Component of A, d) Image A in La*b* Color Space

In Figure 7.11, the given test image A, is shown in La*b* color space after transforming from RGB color space within the transformation process which is mentioned in chapter 5. As it can be seen a represents the L or luminosity layer of image A, b shows a* or chromacity layer of given image A, c shows the b*or chromacity layer of given image A and d shows a*b* layers of given image A.

Formation of image B in La*b* space:

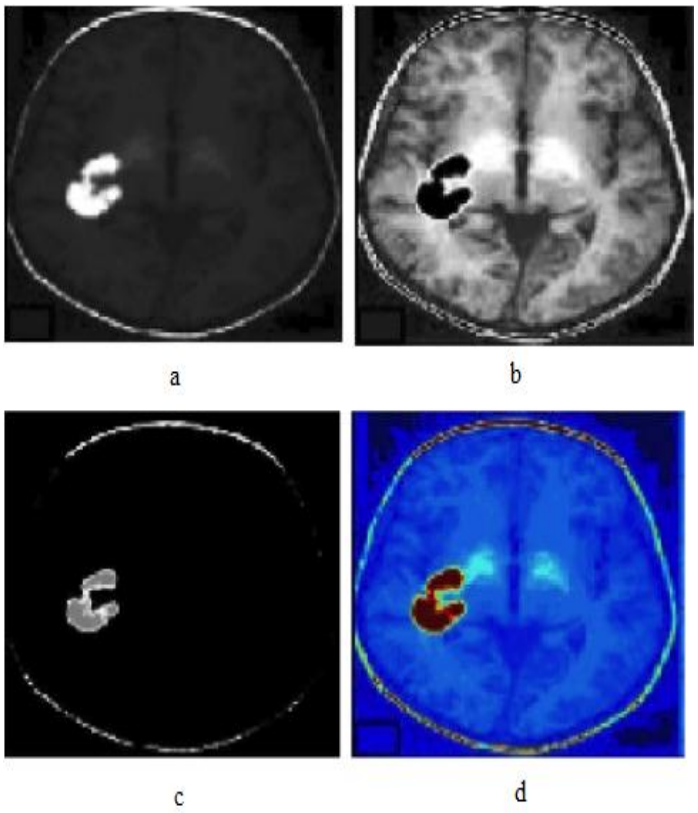

Figure 7. 12: a) L Component of B, b) a* Component of B, c) b* component of B, d) Image B in La*b* Color Space

In Figure 7.12, you can see the given image B in La*b* color space. The luminosity layer of given image shows in a, b shows a* or chromacity layer of image B, c shows the b*, chromacity layer of B and at last d shows a*b* layers of given image B.

Formation of image C in La*b* space:

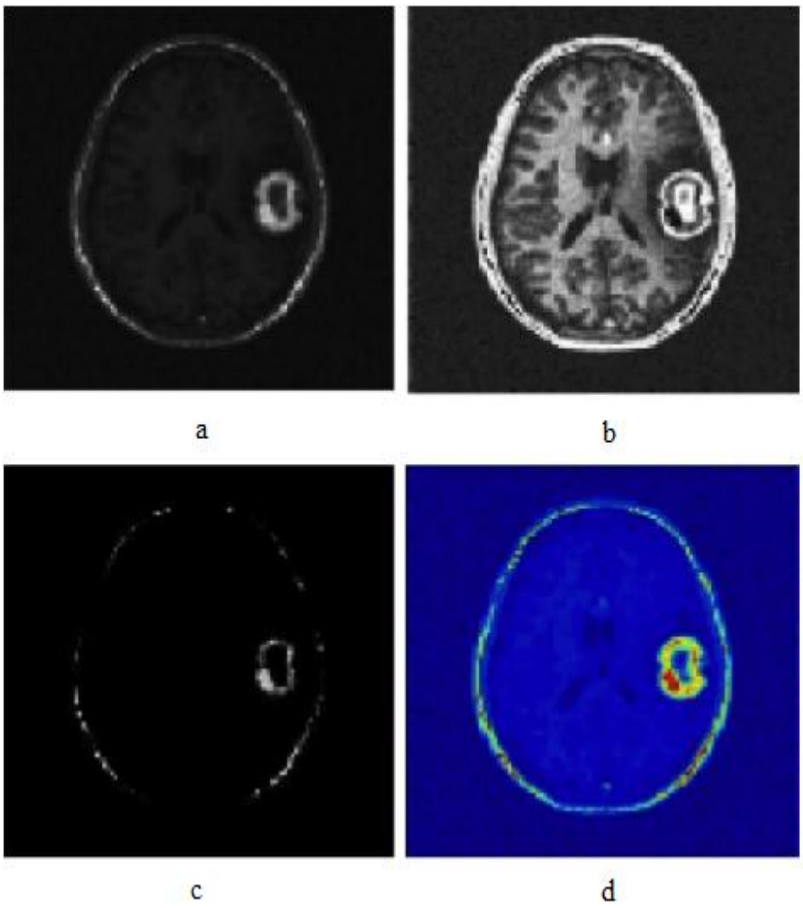

Figure 7. 13: a) L Component of C, b) a* Component of C, c) b* Component of C, d) Image C in La*b* Color Space

Figure 7.13 indicates the given test image C in La*b* color spae. Luminosity layer of image C is shown in a, while b shows a*, chromacity layer of given image C,b shows b* chromacity leayer of image C and d shows a*b* layers of given image C. After extracting L, a* and b* component of input images, next step is to apply a* and b* layers of given test image A, in K-Means segmentation algorithm to be segmented to n number of clusters. The process will be explained in 7.4 section as well.

7.4 K-Means Based MRI Brain Image Segmentation

Having T1 brain images inverted to La*b* color images, they are prepared to image segmentation. The important deal in this section is to classify pseudo-colored images into clusters by means of K-Means algorithm. As is mentioned in chapter 3, the

scenario which we used in this thesis includes some steps finally results in extracting lesion region segmented from other regions of an image.

The first step is to input brain T1 image with lesion region and change it to gray-scale, simply shown in Figure 7.14. As it can be seen, a is a gray-scale of given image A, b shows the image A in HSI color space and c shows a*b* layers of image A in color space.

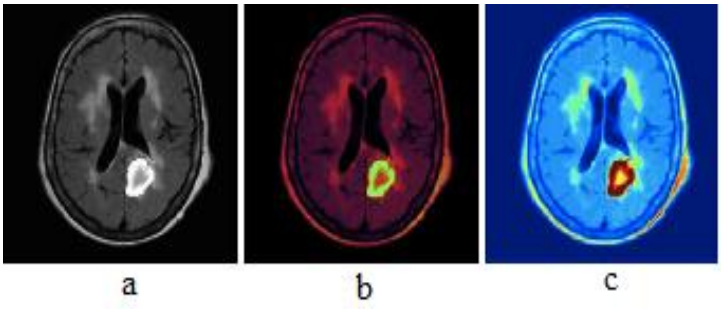

Figure 7. 14: a) Input Gray-Scale Test Image, b) Converted Image in HSI, c) Converted Image in La*b*

The next step is to classify La*b* image into clusters. k-means segmentation algorithm classifies the given a*b* image into n number of clusters. The number of clusters can be chosen manually within corresponding matlab code . Here in this test choosen number of clusters is 5 so there are five different clusters shown in Figure 7.15. In this figure a shows the segmented image A by K-Means, a-d shows the four random different clusters of given image A, e shows the chosen segmented cluster which contains the region of interest, tumor, f shows brain mask used to eliminate extra and unwanted parts of brain, g shows the segmented tumor region of given image A,h shows segmented tumor region with green edge contour, and i finally shows given T1w brain image A with segmented tumor region on it.

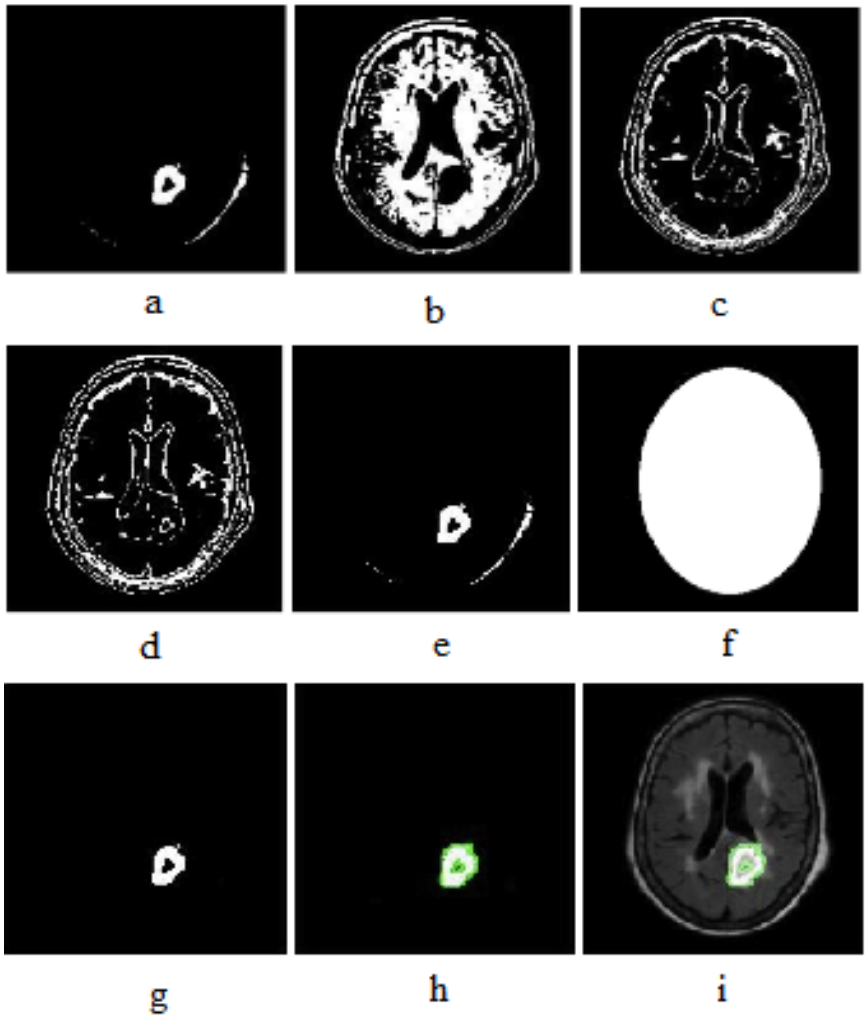

Figure 7. 15: a-d) Different Segmented Clusters using K-Means, e) Chosen Segmented Cluster, f) Brain Mask Used for Post-Processing, g) Extracted Tumor Region, h) Tumor Region with Green Edge Contour, i) Output Test Image with Segmented Tumor Region

7.5 FCM Based MRI Brain Image Segmentation

In this episode the segmentation have been done by means of the proposed image segmentation algorithm FCM or Fuzzy C-Means. This time a*b* layers of test image calculated in previous sections, is applied to FCM segmentation method to be classified in n number of clusters. Like K-Means method, n is an arbitrary number, which defines the number of desired clusters that is chosen by user. In this thesis initial values, which are chosen for FCM algorithm are $m=2, \varepsilon = 0.1$ and 100 iteration. The proposed method segmented the given test image into number of

clusters. Among different clusters we are able to choose the desired cluster with tumor part in it. After finding best cluster, it is necessary to do post-processing to clean other non-important regions in image. To show the tumor region we apply a morphological dilation, which sketches the green edge contour around tumor region and finally again we add this region to initial image. As the results in Figure 7.16, show a-d are four different chosen segmented clusters, e shows the chosen segmented cluster, f shows the brain mask to eliminate unwanted regions of brain, g shows the complete segmented tumor part, h shows the tumor region with green edge contour and i shows the input test image with segmented tumor on it.

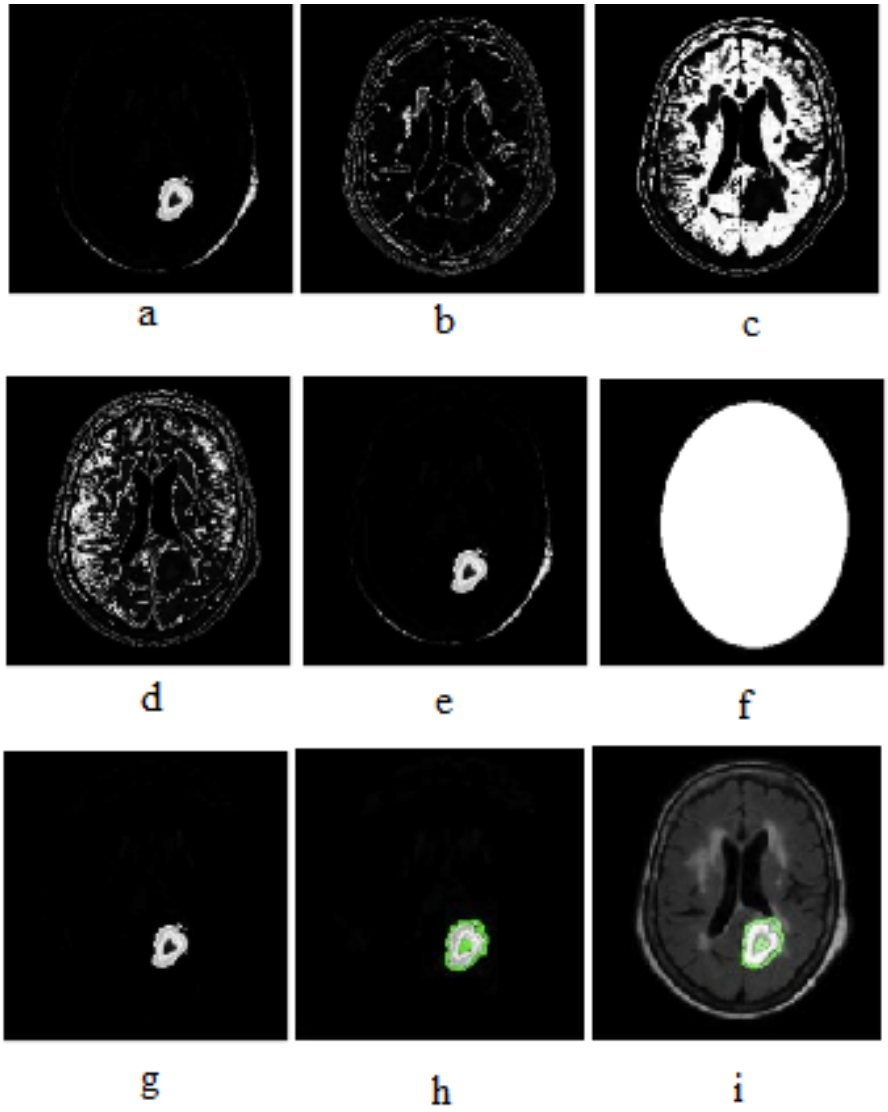

Figure 7. 16: a-d) Different Segmented Clusters using FCM with m=2, $\varepsilon = 0.1$, e) Chosen Segmented Cluster, f) Brain Mask Used for Post-Processing, g) Extracted Tumor Region, h) Tumor Region with Green Edge Contour, i) Output Test Image with Segmented Tumor Region

As the results indicate, it is obvious that tumor region is highlighted precisely with this proposed method.

7.6 Visual Results

To show the performance of our proposed segmentation method in this episode, K-Means and Fuzzy C-Means segmentation algorithm have been applied to three different types of T1w abnormal brain images. The first image is a real T1w brain

image with a tumor region, second is the synthetic T1w Brain image with tumor, which is generated by others in this paper [7] and the last one is our own synthetic T1w brain image, which is came out through synthetic generation process that is explained in 7.3.1 previously. The results of given three dataset of both k-means and fuzzy c-means algorithms, can be seen in this figure. As you can see the performance of k-means (Figure 7.17) and our proposed method, FCM, (Figure 7.18) clearly is depicted by means of visual results of two methods. The segmented tumor region is shown in each image results.

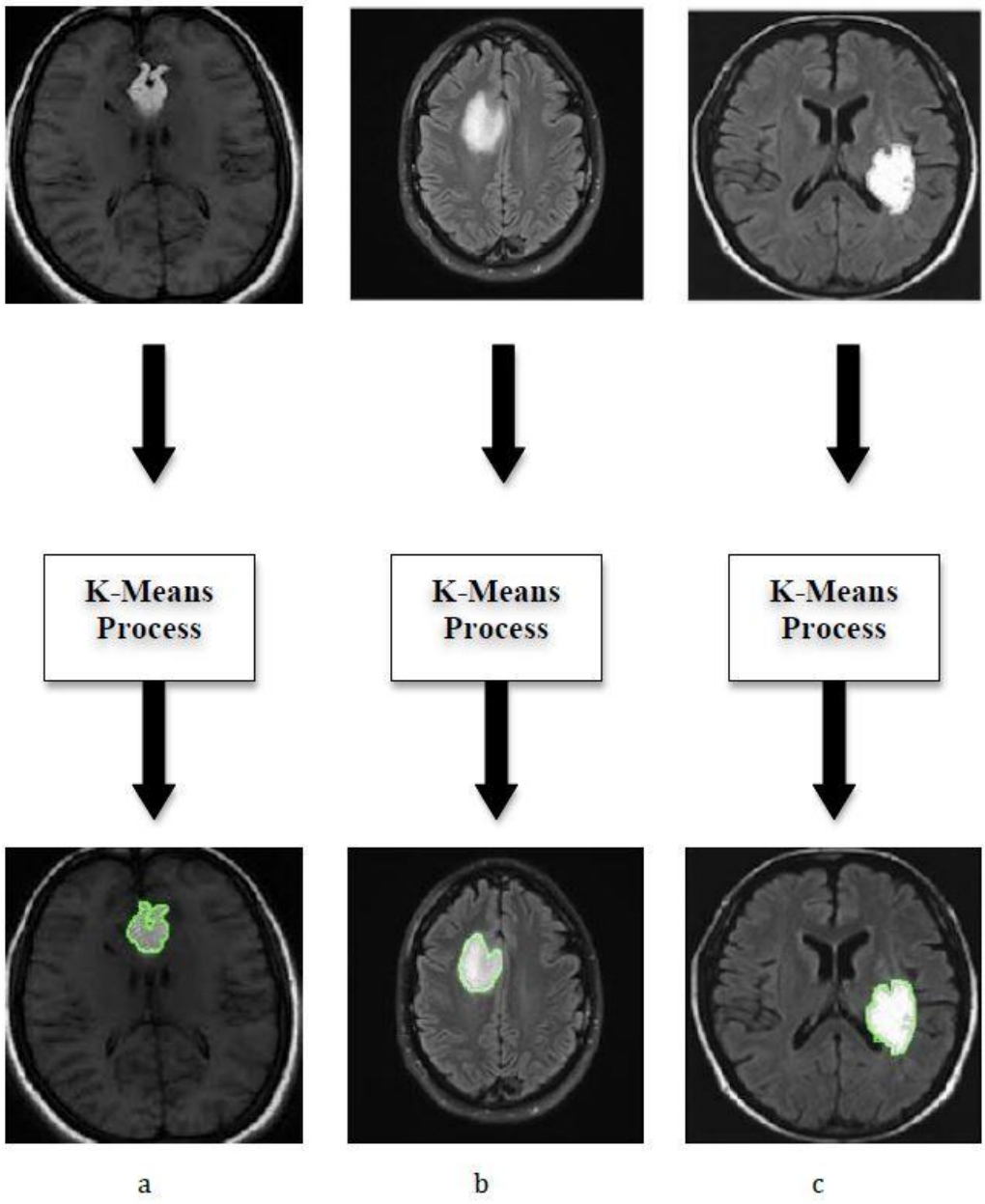

Figure 7. 17: a) Real T1w Abnormal Brain Image, b)Synthetic T1w Abnormal Brain Image Generated by [7] , c) Our Synthetic T1w Abnormal Brain Images, all Segmented using K-Means Algorithm

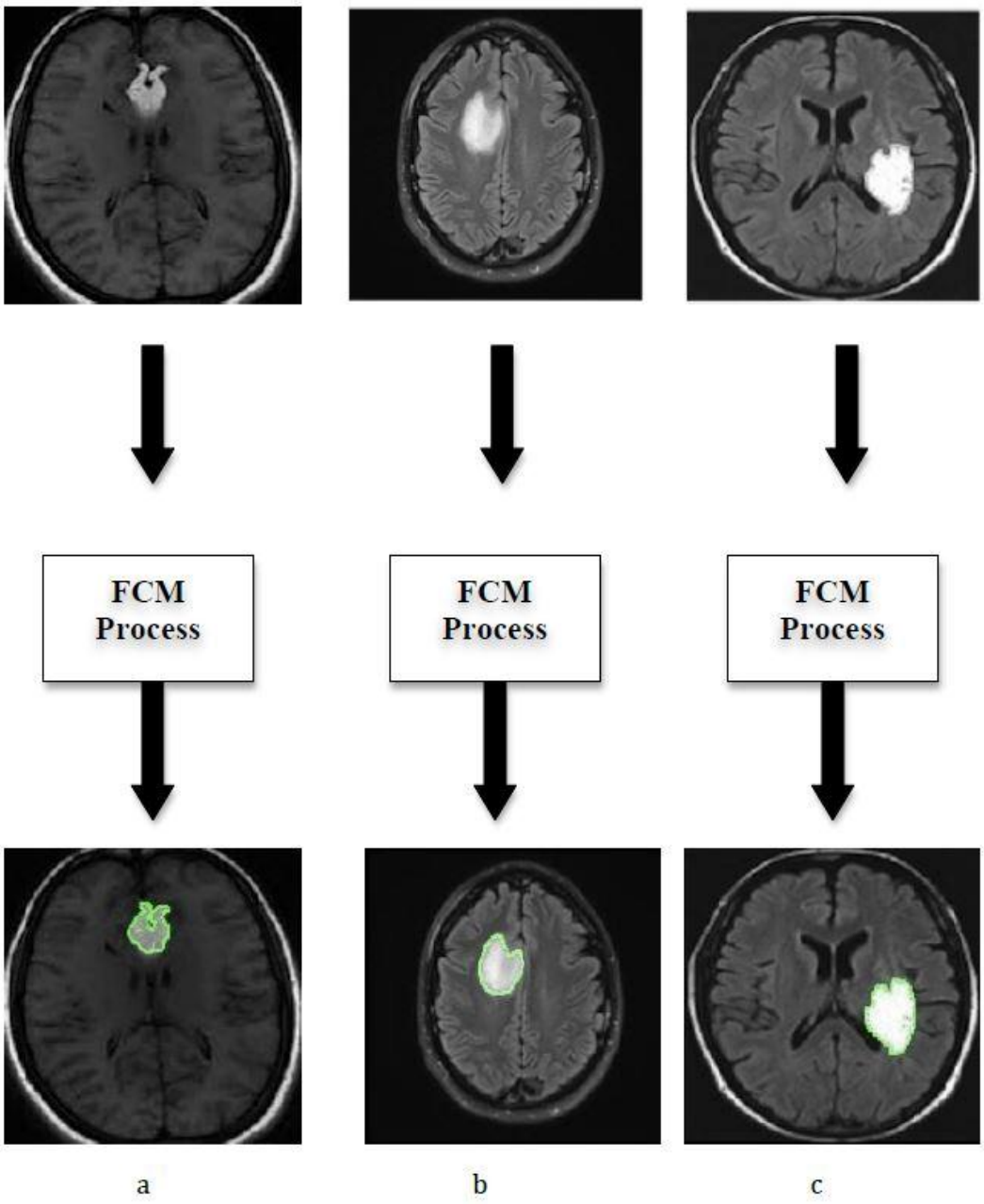

Figure 7. 18 : a) Real T1w Abnormal Brain Image, b)Synthetic T1w Abnormal Brain Image Generated by [7] , c) Our Synthetic T1w Abnormal Brain Images, all Segmented using FCM Algorithm with m=2, $\varepsilon = 0.1$

7.7 System Accuracy Analysis

Although, visual results can depict the performance of one method more clearly but again there are some important information that may be missed. Unlike visual results, statistic results carry more information of each dataset by means of some useful standard metrics. The chosen metric for each dataset depends on type of

processing which is carried on in each test. Since this thesis deals with image processing, we have to choose special metric for this type of processing. As mentioned before, chosen metrics for this thesis, are: sensitivity, precision, Structural Similarity Index Measurement or SSIM, peak signal to noise ratio or PSNR and segmentation accuracy. Here, we calculate all these parameters for each five test groups in two episodes, one for applied K-Means algorithm and one for our proposed fuzzy c-means algorithm. The tables of results for each applied algorithm can be seen in 7.6.1 and 7.6.2 parts.

7.7.1 K-Means Accuracy Results

In this episode, we obtain k-means segmentation algorithm to segment our test data set, then we evaluate the performance of used algorithm by means of Sensitivity, precision, SSIM, PSNR and segmentation measurements. Their corresponding formulas are explained in part 7.2, experimental methodology as well. As you see, Table 7.1 includes the sensitivity, precision, SSIM, PSNR and segmentation accuracy results of test image group 1 using k-means algorithm.

Table 7.1: K-Means Results for Dataset Images, Group 1

Group 1	Sensitivity%	Precision%	SSIM	PSNR(dB)	Segmentation Accuracy%
Image 1	100.00	99.00	0.9968	69.95	100.00
Image 2	98.00	99.00	0.9970	70.93	98.00
Image 3	87.00	99.00	0.9972	68.59	87.00
Image 4	81.00	99.00	0.9967	71.22	81.00
Image 5	77.00	99.00	0.9967	62.14	77.00
Average	88.60	99.00	0.9968	68.56	88.60

Table 7.2, shows sensitivity, precision, SSIM, PSNR and segmentation accuracy results of test image group 2 using K-Means algorithm

Table 7.2: K-Means Results for Dataset Images, Group 2

Group 2	Sensitivity%	Precision%	SSIM	PSNR(dB)	Segmentation Accuracy%
Image 1	86.00	99.00	0.9955	68.66	86.00
Image 2	69.00	99.00	0.9958	66.77	69.00
Image 3	86.00	99.00	0.9960	67.93	86.00
Image 4	65.00	99.00	0.9959	68.94	65.00
Image 5	72.00	99.00	0.9962	64.92	72.00
Average	75.60	99.00	0.9958	67.44	75.60

Table 7.3, shows sensitivity, precision, SSIM, PSNR and segmentation accuracy results of test images group 3 using K-Means algorithm.

Table 7.3: K-Means Results for Dataset Images, Group 3

Group 3	Sensitivity%	Precision%	SSIM	PSNR(dB)	Segmentation Accuracy%
Image 1	46.00	97.00	0.9961	71.28	46.00
Image 2	81.00	98.00	0.9963	73.16	81.00
Image 3	56.00	96.00	0.9958	66.71	56.00
Image 4	68.00	98.00	0.9958	72.79	68.00
Image 5	96.00	99.00	0.9957	66.08	96.00
Average	69.50	98.00	0.9959	70.00	69.50

Table 7.4, shows sensitivity, precision, SSIM, PSNR and segmentation accuracy of test images group 4 using K-Means algorithm.

Table 7.4: K-Means Results for Dataset Images, Group 4

Group 4	Sensitivity%	Precision%	SSIM	PSNR(dB)	Segmentation Accuracy%
Image 1	70.00	95.00	0.9966	67.32	70.00
Image 2	93.00	99.00	0.9969	69.08	93.00
Image 3	88.00	99.00	0.9963	68.37	88.00
Image 4	86.00	99.00	0.9969	66.88	86.00
Image 5	90.00	99.00	0.9962	66.27	90.00
Average	85.40	97.00	0.9965	67.58	85.40

Finally Table 7.5, indicates sensitivity, precision, SSIM, PSNR and segmentation accuracy of test images group 5 using K-Means algorithm.

Table 7.5: K-Means Results for Dataset Images, Group 5

Group 5	Sensitivity%	Precision%	SSIM	PSNR(dB)	Segmentation Accuracy%
Image 1	58.00	98.00	0.9956	70.43	58.00
Image 2	97.00	99.00	0.9961	74.13	97.00
Image 3	71.00	98.00	0.9964	70.31	71.00
Image 4	91.00	99.00	0.9959	73.02	91.00
Image 5	95.00	99.00	0.9955	66.13	95.00
Average	82.50	98.60	0.9958	70.80	82.50

7.7.2 FCM Accuracy Results

In this episode, we apply our proposed segmentation algorithm on test data set subsequently the evaluation of our proposed method is done by aid of five standard metrics namely are sensitivity, precision, SSIM, PSNR and segmentation accuracy. The related formulas are mentioned in experimental methodologies part. As it can be seen Table 7.6 carries the sensitivity, precision, SSIM, PSNR and segmentation

accuracy results of test image group 1 this time by applying our proposed method Fuzzy C-Means method when m=2, $\varepsilon = 0.1$.

Table 7.6: FCM Results for Dataset Images, Group 1

Group 1	Sensitivity%	Precision%	SSIM	PSNR(dB)	Segmentation Accuracy%
Image 1	100.00	98.00	0.9973	75.13	100.00
Image 2	99.00	98.00	0.9975	76.25	99.00
Image 3	99.00	98.00	0.9972	71.12	99.00
Image 4	100.00	98.00	0.9974	75.48	100.00
Image 5	100.00	99.00	0.9974	66.25	100.00
Average	99.60	98.20	0.9973	72.84	99.60

Table 7.7 includes information of four metric, sensitivity, precision, SSIM, PSNR and segmentation accuracy results of test images group 2 after applying our proposed segmentation algorithm Fuzzy C-Means algorithm.

Table 7.8 shows results of sensitivity, precision, SSIM, PSNR and segmentation accuracy metric of test images group 3 applying our proposed segmentation method, Fuzzy C-Means method.

Table 7.7: FCM Results for Dataset Images, Group 2

Group 2	Sensitivity%	Precision%	SSIM	PSNR(dB)	Segmentation Accuracy%
Image 1	98.00	98.00	0.9975	72.43	98.00
Image 2	97.00	98.00	0.9977	69.5	97.00
Image 3	97.00	98.00	0.9976	71.01	97.00
Image 4	99.00	98.00	0.9979	74.28	99.00
Image 5	100.00	98.00	0.9974	68.75	100.00
Average	98.20	98.00	0.9976	71.19	98.20

Table 7.8: FCM Results for Dataset Images, Group 3

Group 3	Sensitivity%	Precision%	SSIM	PSNR(dB)	Segmentation Accuracy%
Image 1	99.00	99.00	0.9983	75.24	99.00
Image 2	98.00	99.00	0.9980	77.60	98.00
Image 3	100.00	99.00	0.9984	72.13	100.00
Image 4	99.00	99.00	0.9980	69.01	99.00
Image 5	97.00	99.00	0.9982	75.30	97.00
Average	98.60	99.00	0.9981	73.85	98.60

Table 7.9 contains results of four sensitivity, precision, SSIM, PSNR and segmentation accuracy metrics for test images group 4 after obtaining our proposed segmentation method Fuzzy C-Means method.

Finally Table 7.10 shows results of sensitivity, precision, SSIM, PSNR and segmentation accuracy standards for test images group 5 using our proposed segmentation algorithm, Fuzzy C-Means algorithm.

Table 7.9: FCM Results for Dataset Images, Group 4

Group 4	Sensitivity%	Precision%	SSIM	PSNR(dB)	Segmentation Accuracy%
Image 1	100.00	99.00	0.9978	70.76	100.00
Image 2	99.00	98.00	0.9973	71.72	99.00
Image 3	97.00	99.00	0.9977	73.24	97.00
Image 4	99.00	98.00	0.9979	69.90	99.00
Image 5	99.00	98.00	0.9974	69.18	99.00
Average	98.80	98.40	0.9975	70.96	98.80

Finally Table 7.10 shows results of sensitivity, precision, SSIM, PSNR and segmentation accuracy standards for test images group 5 using our proposed segmentation algorithm, Fuzzy C-Means algorithm.

Table 7.10: FCM Results for Dataset Images, Group 5

Group 5	Sensitivity%	Precision%	SSIM	PSNR(dB)	Segmentation Accuracy%
Image 1	100.00	99.00	0.9976	73.56	100.00
Image 2	98.00	99.00	0.9978	79.60	98.00
Image 3	97.00	99.00	0.9974	76.81	97.00
Image 4	99.00	99.00	0.9977	78.32	99.00
Image 5	97.00	99.00	0.9975	73.54	97.00
Average	98.20	99.00	0.9976	76.36	98.20

7.8 Comparison between FCM and K-Means

To indicate the performance of two used segmentation algorithms, K-Means and proposed Fuzzy C-Means, we tried to show the comparison of calculated results of our test image groups by means of graphs and charts. The graphs clearly indicate reliability and preision of our proposed segmentation. Figure 7.19 shows comparison of two applied segmentation algorithms of all image groups 1-5 according their average sensitivity percentages. Line red corresponds to average sensitivity percentages using K-Means and blue line corresponds to average sensitivity percentages of different test image groups using our proposed Fuzzy C-Means algorithm. It can be seen that in test image groups segmented by Fuzzy C-Means algorithm, average sensitivity changes steadily around 100. In test images segmented by K-Means average sensitivity shows a fluctuation between 70 and 90 percent.

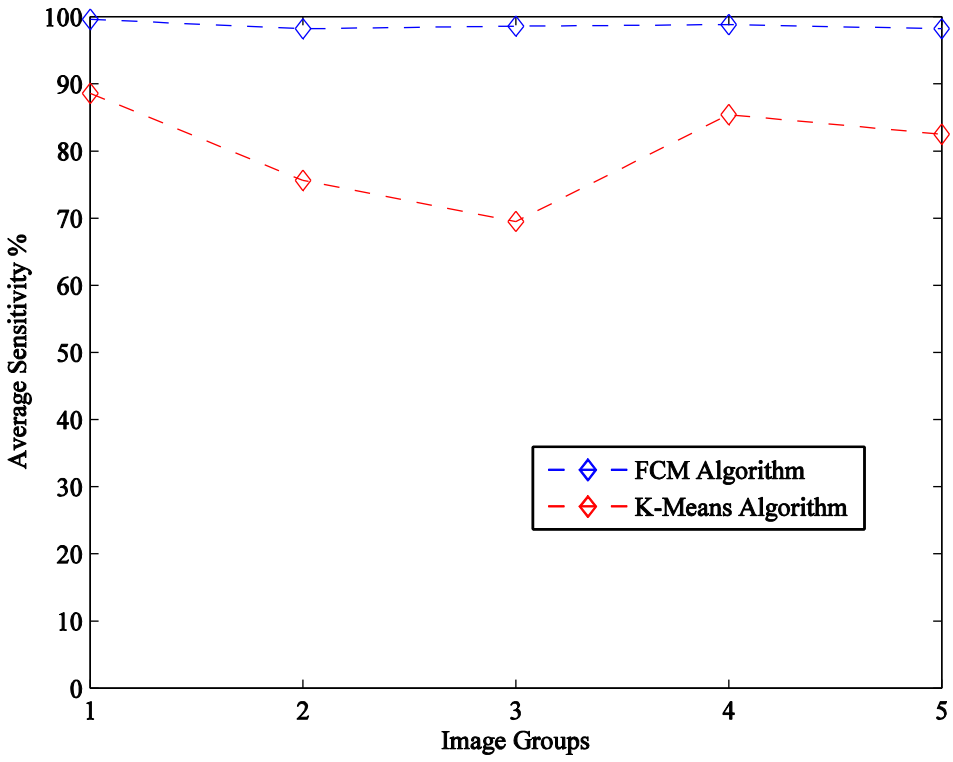

Figure 7. 19: Comparison of Average Sensitivity Percentage of Dataset for K-Means & FCM Algorithms, m=2, $\varepsilon = 0.1$

Graph 7.20 shows the comparison of average precision percentages among five different test image groups 1-5 for two used segmentation algorithms. In this figure, red line relates to result of K-Means algorithm and blue line relates to results of Fuzzy C-Means algorithm. In precision comparison two used segmentation algorithm show approximately same precision percentages. Both blue and red lines have a steady mood between 98 and 99 percents.

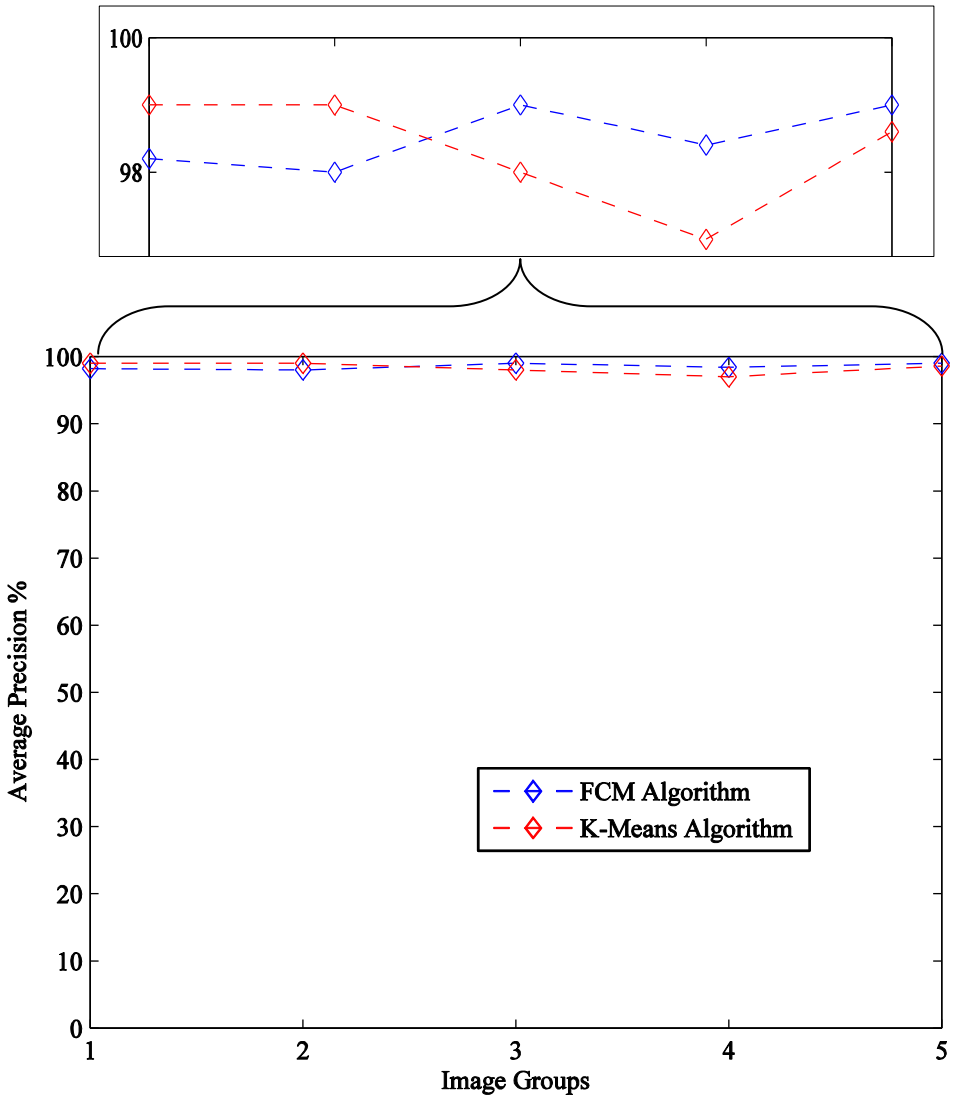

Figure 7. 20 : Comparison of Average Precision percentage of Dataset for K-Means & FCM Algorithms with m=2, $\varepsilon = 0.1$

Here, Figure 7.21, shows the comparison of average SSIM results for five different test image groups of two applying algorithms, K-Means and proposed Fuzzy C-Means. As you can see red line, represent SSIM results of applied K-Means algorithm, reach its highest amount 0.9969 belonging to image group 3, while blue line of FCM method has the maximum point in 0.9981 belongs to image group 4. The minimum SSIM of K-Means results belongs to image group 4 with amount of 0.9958 meanwhile, lowest SSIM for FCM algorithm is seen in image group 5 with percentage of 0.9973.

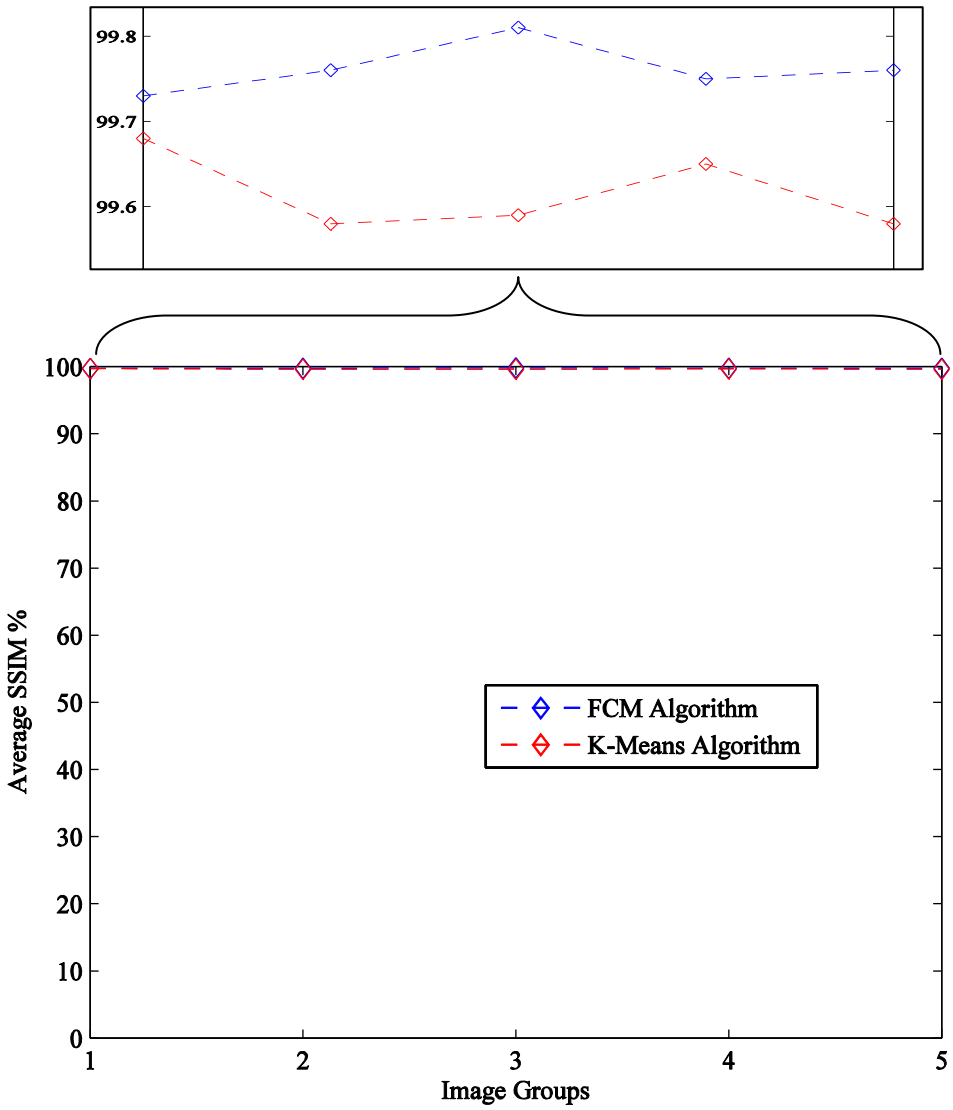

Figure 7. 21: Comparison of Average SSIM percentage of Dataset for K-Means & FCM Algorithms with m=2, $\varepsilon = 0.1$

In Figure 7.22, the average PSNR percents for five different image groups of K-Means and FCM segmentation algorithms can be seen easily. Both segmentation methods Show fluctuation between 65 and 75 percents. Blue line stands for PSNR results for FCM shows higher average PSNR at all five image groups. Conversely, red line, which stands for PSNR results of K-Means method, has lower PSNR percents.

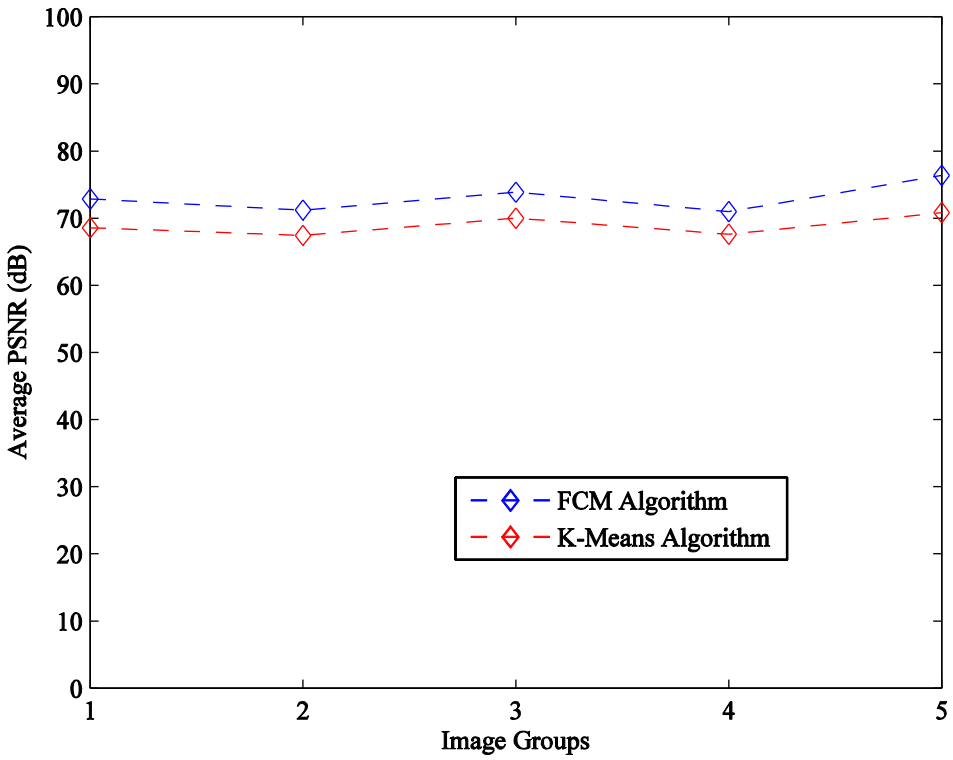

Figure 7. 22: Comparison of Average PSNR percentage of Dataset for K-Means & FCM Algorithms with m=2, $\varepsilon = 0.1$

Figure 7.23 shows the comparison of two applied segmentation algorithms, k-means and FCM, among five different test image groups according their average segmentation accuracy. It is clear that red line, K-Means results, has the lowest point 69.5 in image group 3 and it reaches to its peak in point 88.6 coming from image group 5. On the other hand, blue line for FCM results changes steadily around 98 percent. In overall results of our proposed method are better than other method.

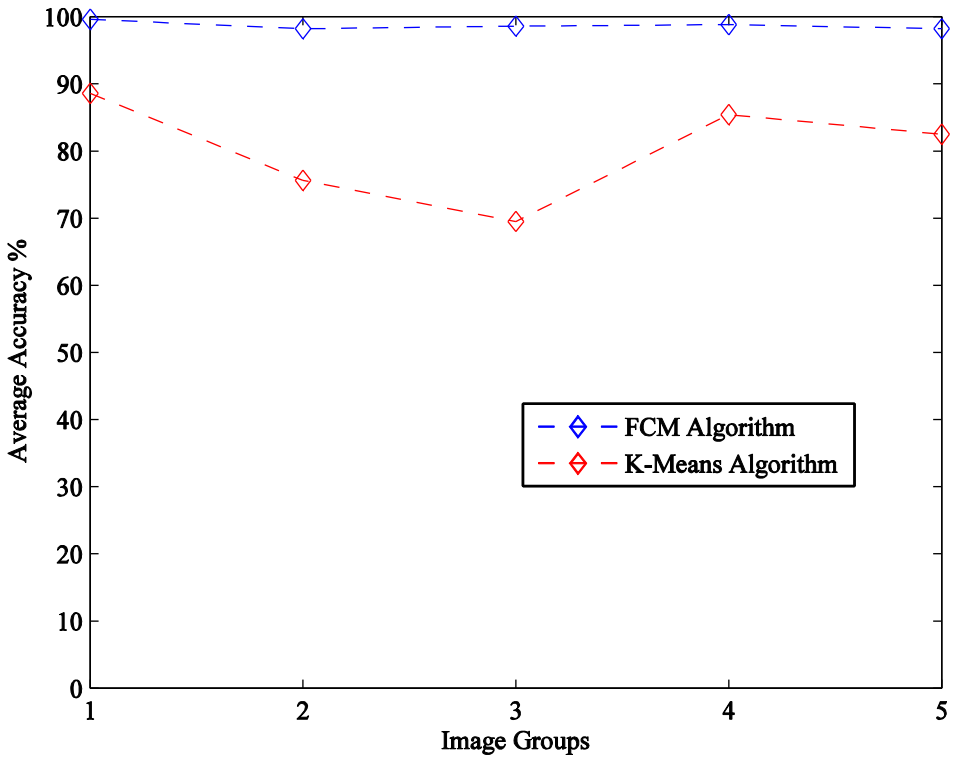

Figure 7. 23: Comparison of Average Accuracy percentage of Dataset for K-Means & FCM Algorithms with m=2, $\varepsilon = 0.1$

Here there are five charts compare the PSNR of each test images in each five groups after applying two K-Means and FCM segmentation algorithms. The comparison of two methods can be seen clearly in five charts. In Figure 7.24, the performance of two methods is shown with two blue and red colors. The blue one, which belongs to FCM method, is higher than yellow one, K-Means method, in all five tests images of image group 1.

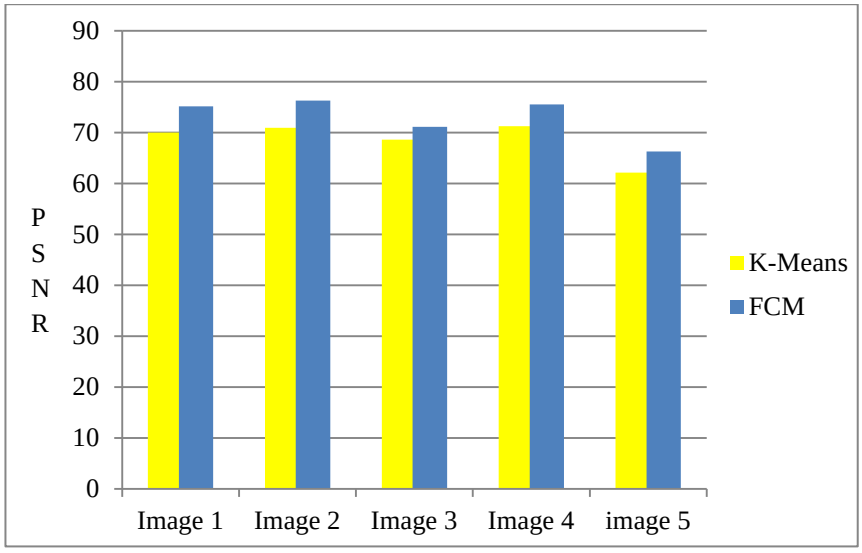

Figure 7. 24: PSNR Comparison of K-Means & FCM Results for Image Group1

Figure 7.25, compares results of PSNR metric coming from image group 2 after using K-Means and FCM segmentation methods by means of two blue and yellow colors. Like the previous chart, blue one related to FCM method indicates higher PSNR results in each image in this group.

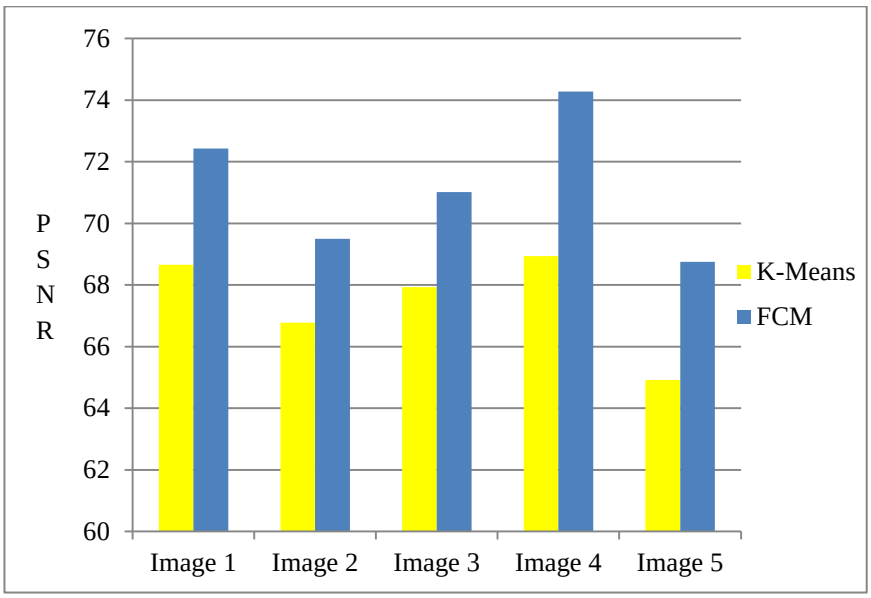

Figure 7. 25: PSNR Comparison of K-Means & FCM Results for Image Group2

Figure 7.26, indicates the PSNR of each image in group 3 comparing two K-Means and FCM segmentation methods. Like previous charts, this chart shows the same results, higher PSNR of each image of group 3.

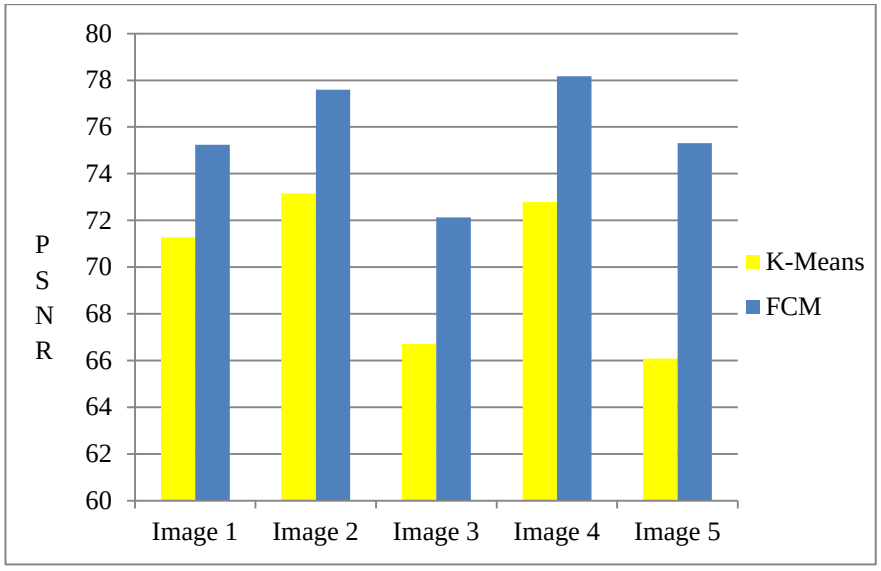

Figure 7. 26: PSNR Comparison of K-Means & FCM Results for Image Group3

Figure 7.27, presents the comparison of two applied segmentation algorithms in image group 4 according their PSNR by means of two blue and yellow colors. As it can be seen, PSNR results of K-Means method in yellow color are lower than PSNR results of FCM method in blue color.

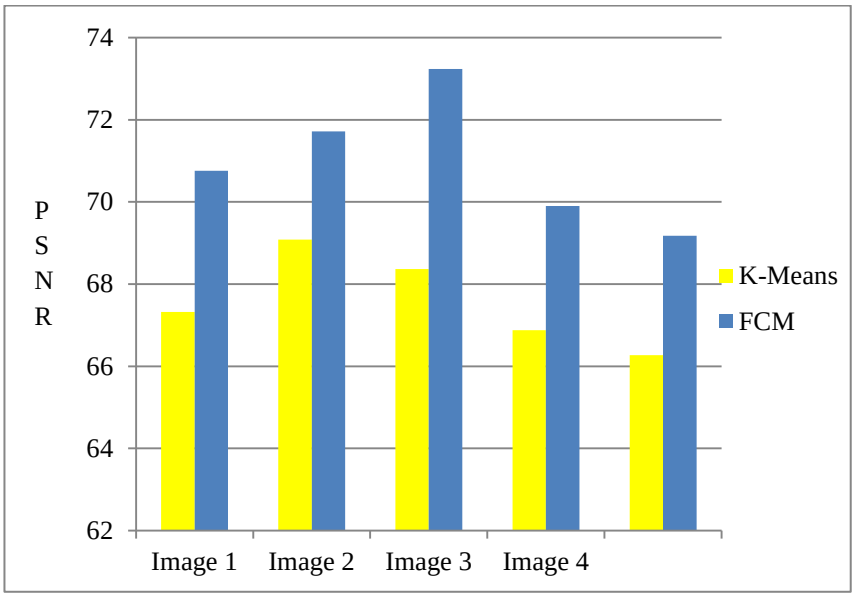

Figure 7. 27: PSNR Comparison of K-Means & FCM Results for Image Group4

Figure 7.28, presents the comparison of PSNR results of two K-Means and FCM methods of each image in image group 5. The difference between both methods,

clearly show by blue and yellow colors. Like other groups PSNR results of FCM are higher than other method.

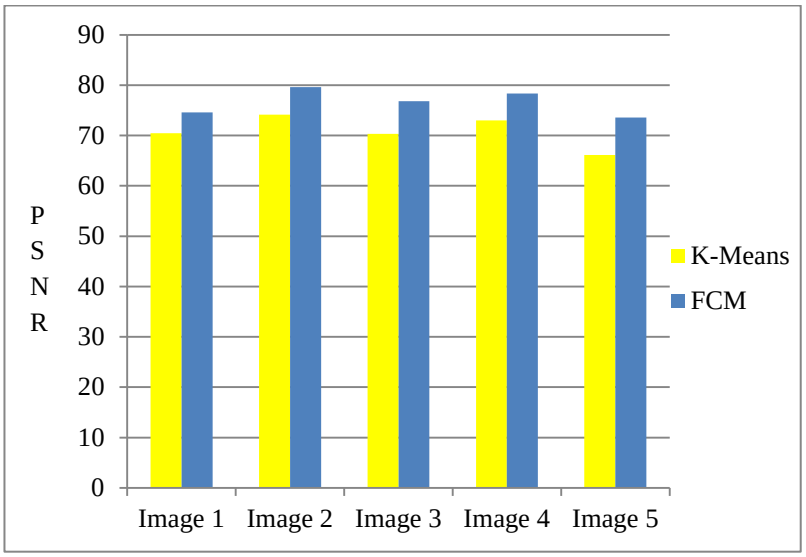

Figure 7. 28: PSNR Comparison of K-Means & FCM Results for Image Group5

7.9 Cluster Analysis of two Methods

In this episode we tried to show the changing sensitivity rate of two used methods by changing the number of cluster in each method. Figure 7.29, shows the performance of two methods in four chosen number of clusters, 3, 5, 7 and 10. Red line is for K-Means and Blue is for our proposed FCM. As you can see, the sensitivity rate for used FCM method is higher than K-Means method by changing cluster numbers. By increasing cluster numbers sensitivity rate in FCM is increasing, while in K-Means algorithm, increasing numbers of cluster subsides sensitivity rate.

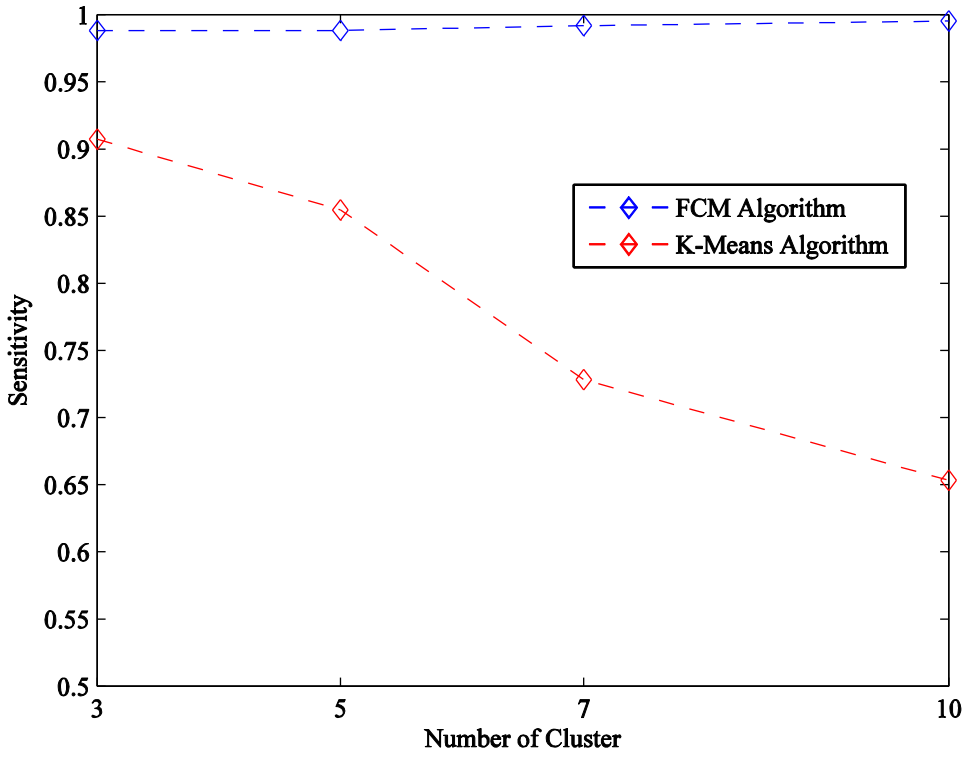

Figure 7. 29: Comparison of K-Means & FCM Algorithms(m=2, $\varepsilon = 0.1$) According to Sensitivity

In Figure 7.30, we tried to show the changing precision of two methods by increasing the cluster numbers. As seen here, FCM method holds higher precision rate than K-Means up to number of cluster 7. When number of cluster increases to 10, precision rate of FCM method falls to 0.9889 while the precision of k-means method is in 0.9944.

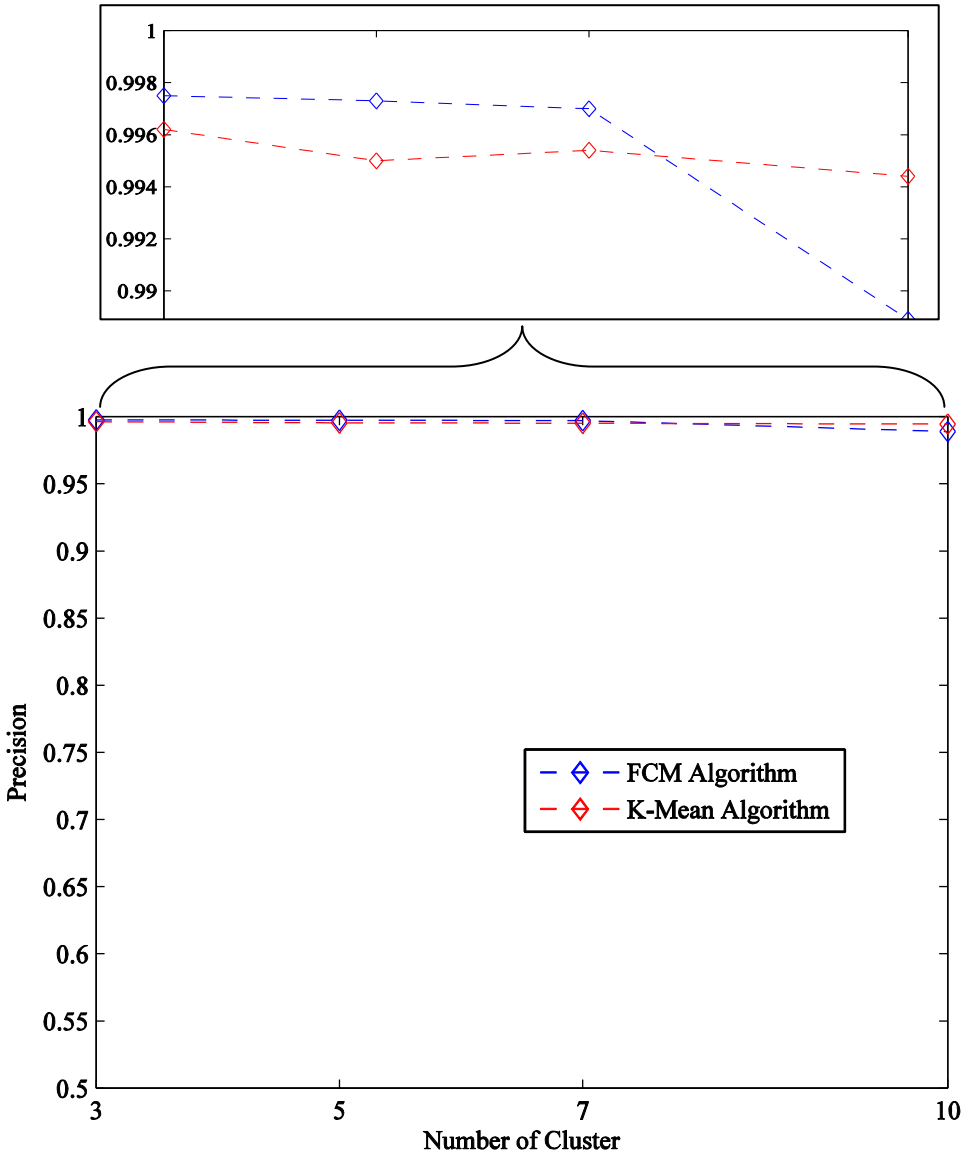

Figure 7. 30: Comparison of K-Means & FCM Algorithms(m=2, $\varepsilon = 0.1$) According to Precision

In Figure 7.31, you can see the comparison of SSIM rates of two methods by increasing number of clusters in each method.In both methods SSIM rate is decreasing when the number of cluster goes up. When cluster number is 10, SSIM of both blue and red graphs are decreasing. Again FCM method has better results in general.

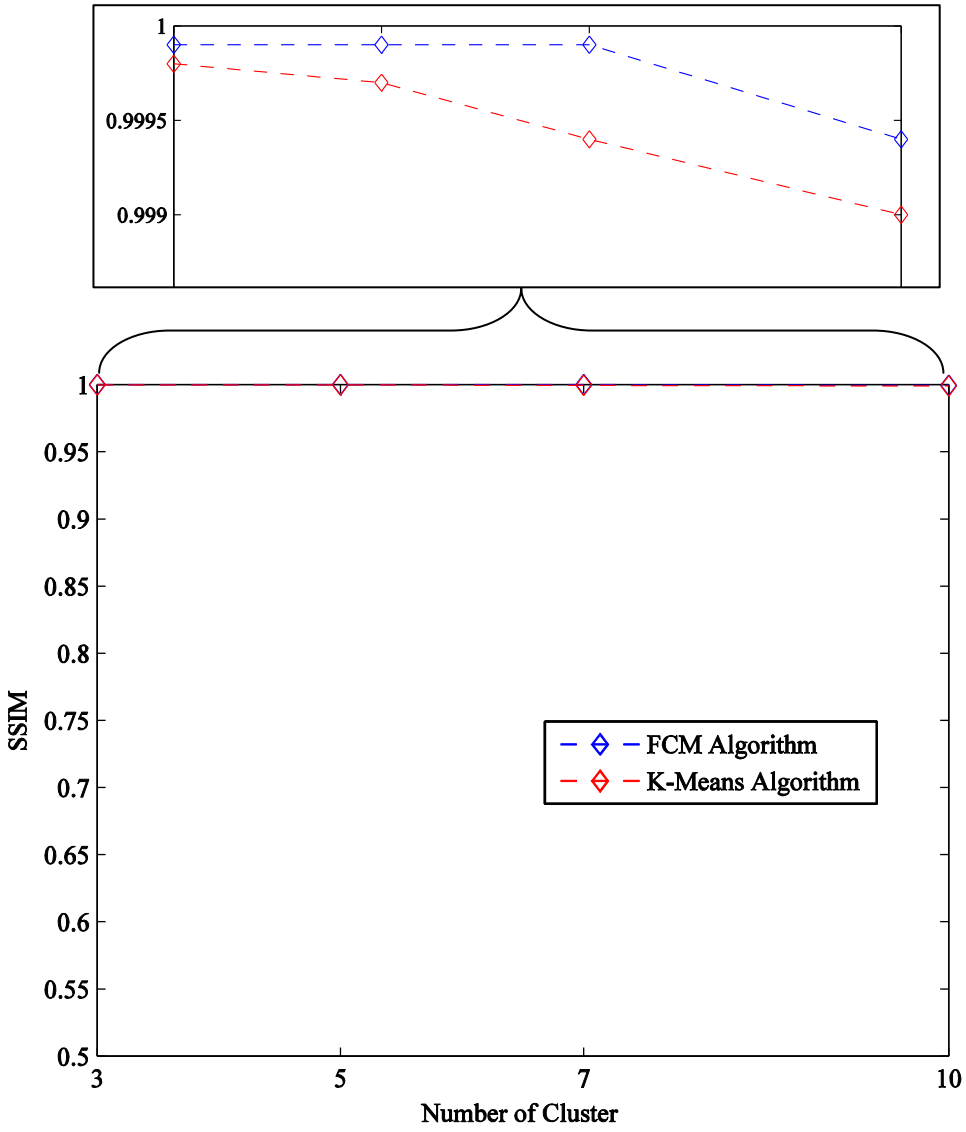

Figure 7. 31: Comparison of K-Means & FCM Algorithms(m=2, $\varepsilon = 0.1$) According to MSSIM

Figure 7.32, Shows the comparison of PSNR rate of two used method in differen tnumber of clusters. PSNR rate for two used K-Means and FCM Methods hold higher results as number of clusters is 3, 5 and 7. In clusternumber 10, both graphs fall down. Totally FCM shows better performance in PSNR than K-Means.

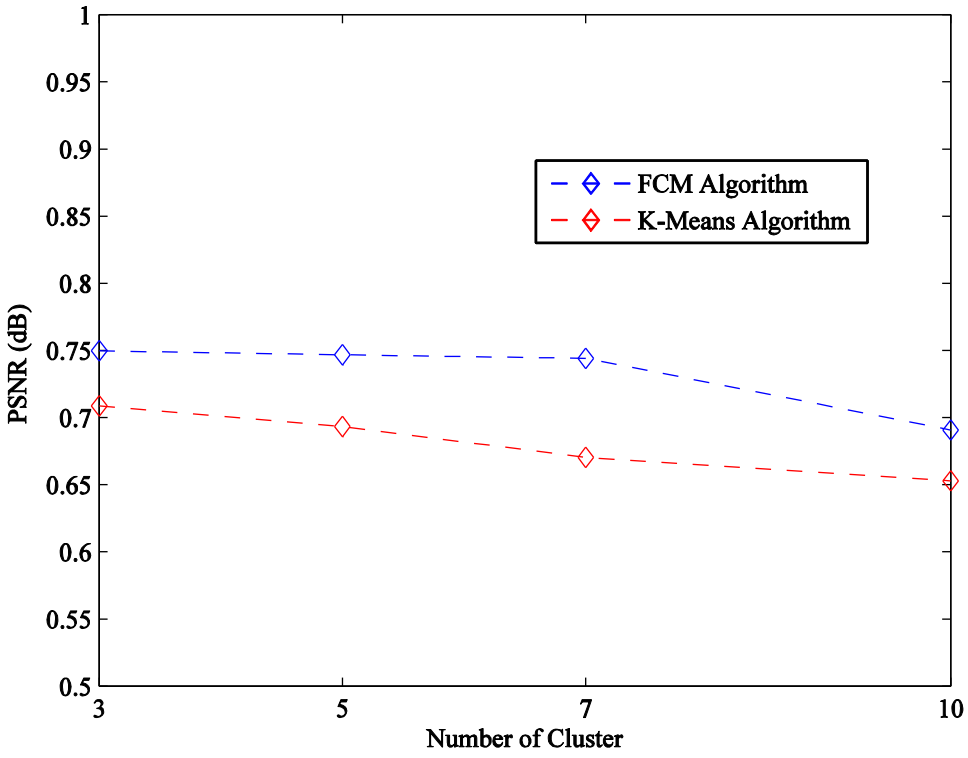

Figure 7. 32: Comparison of K-Means & FCM Algorithms(m=2, $\varepsilon = 0.1$) According to PSNR(dB)

Finally Figure 7.33, compares of segmentation accuracy of two K-Means and FCM methods in different number of clusters: 3, 5, 7 and 10. As it shows in this figure, blue graph corresponds to FCM segmentation method holds higher segmentation accuracy rate in all different number of clusters than K-Means. The FCM segmentation accuracy is going up around 1 while graph of k-means in red, is decreasing as the number of clusters changing. The red graph reaches maximum level 0.9073 when number of cluster is 3.

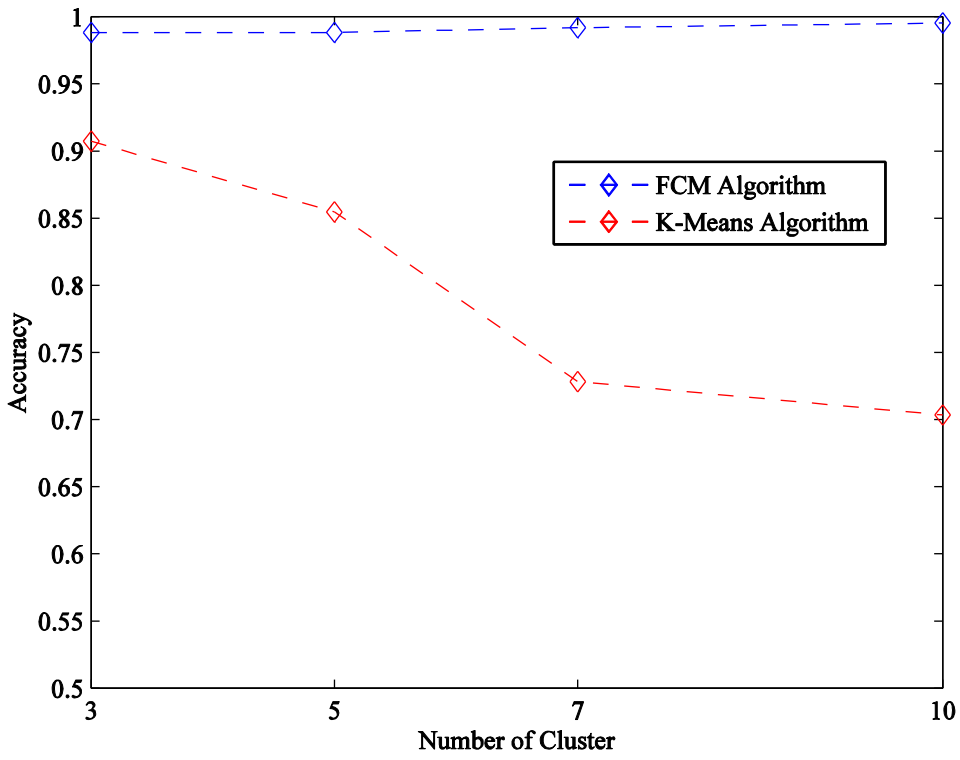

Figure 7. 33: Comparison of K-Means & FCM Algorithms(m=2, $\varepsilon = 0.1$) According Accuracy

The lowest point in K-Means algorithm takes place in cluster number 10 in where the segmentation accuracy is 0.7035. In FCM method, segmentation accuracy reaches to its highest level 0.9952 where the number of cluster is in 10. Finally, according to Figure 7.33, the performance of FCM method is higher than K-Means method.

Chapter 8

CONCLUSIONS

8.1 Conclusion

In this thesis an implementation of pseudo colored segmentation method in detecting tumor region of brain MRI images has been applied to transform input gray-scale T1W brain MRI images with size 255×255, to La*b* color space. Conclusively computed a* and b* compnents, have been sent to two segmentation algorithms namely are K-Means and Fuzzy C-Means to be segmented to different clusters. The big deal is to choose a segmented cluster among all clusters in which the tumor region is segmented from other regions of brain successfuly. To validate performance of both used segmentation methods among test results, ROC (Receiver Operating Characteristic) analysis is performed. The results are taken by means of five standard metrics generally used to evaluate segmentation performance in image segmentation processing. Taken metrics are sensitivity, precision, SSIM, PSNR and segmentation accuracy. Subsequently our preliminary evaluation results in test data set indicates outstanding improvment over on other availabe segmentation methods. Using pesudo-colored FCM segmentation method in order to detect lesion region in MRI brain images is obsereved to have remarkable advantages in clinical applications. The tumor criteria is extracted perfectly from other regions of brain and can be seen clearly with a highkighted edge contour around it. The proposed method

will assist pathalogists to investigate size and region of lesions, tumor or edema precisely.

8.2 Future Work

In future work, the proposed segmentation method could be able to distinguish the type of tumors such as Glioma, Medulloblastoma, Meningioma and other type of brain deformations. Also it could be applied to T2w brain images taken from MRI in pathalogical images as simpley as T1w images by overcoming their short relaxing time and high noise problems. Improvment version of our proposed method will be used by pathalogists to find out the tumor growth step in brain according to its size.

REFERENCES

[1] M. A. Balafar, ABDRahman. Ramli, I. M. Saripan, and R. Mahmud, "Medical Image Segmentation Using Fuzzy C-Means (FCM) and Dominant Grey Levels of Image," *Visual Information Engineering VIE 2008, 5th International Conference* , pp. 314-317, 2008.

[2] S. Shen, W. Sandham, M. H. Granat, M. F. Dempsey, and J. Patterson, "Fuzzy Clustering Based Application to Medical Image Segmentation," *Engineering in Medicine and Biology Society, 2003, Proceedings of the 25th Annual International Conference of the IEEE,* pp. 747-750, 2003.

[3] P.Vasuda, and S. Satheesh, "Improved Fuzzy C-Means Allgorithm for MR Brain Image Segmentation," *International Jornal on Computer Science and Engineering,* vol 02, pp. 1713-1715, 2010.

[4] SJ. He, X. Wng, Y. Yang and W.Yan, "MRI Brain Images Segmentation," *Circuit and System 2000, The 2000 IEEE Asia-Pacific Conferance*, 2000.

[5] N. Rajini, and R. Bhavani, "Enhancing K-means and Kernelized Fuzzy C-Means Clustering with Cluster Center Initialization in Segmenting MRI Brain

Images," *Electronic Computer Technology (ICECT),2011 3rd International Conference*, 2011.

[6] S. R. Kannan, "A new Segmentation System for Brain MR Images Based on Fuzzy Techniques," *Applied Soft Computing for Dynamic Data Mining*, vol 8, no. 4, pp. 1599-1606, 2008.

[7] M. Prastawa, E. Bullitt, and G. Gerig, "Simulation of Brain Tumors in MR Images for Evaluation of Segmentation Efficiency," *Includes Special Section on Functional imageing and Modelling of the heart*, vol 13, no. 2, pp. 297-311, 2009.

[8] C. Carson, S. Belongie, H. Greenspan, and J. Blobworld, "Image Segmentation using Expectation-maximization and its application to image querying," *Digital Object Identifier*, vol 24, no. 8, pp. 1026-1038, 2002.

[9] Y. Su, and X. Song, "Normalized cuts and image segmentation," Retrieved in october 2000, pp.11-15, 2000.

[10] J. Huang, "Segmentation based image comparison," Stanfor publication,vol

03,pp.115-120,2009.

[11] K. S. Fu, and K. J. Mui, "A survey on Image Segmentation Through Clustering," vol 13, no. 1, pp. 3-16, 1981.

[12] Rajagopal, and Venugopal, "Image Segmentation by Histogram Thresholding," vol 10, pp.14-18,2010.

[13] H. Neoh, and A. Hazanchuk, "Adaptive Edge Detection for Real-time Video Processing using FPGAs," *Global Signal Processing*, 2004.

[14] O. R. P. Direne, A. I, and L. Silva, "Edge Detection to Guide Range Image Segmentation by Clustering Techniques," vol 25, no.2, pp.114-118, 1999.

[15] Y. Xiaohan, and J. Yla-Jaaski, "Image Segmentation Combining Region Frowing and Edge Detection," *Image,Speech and Signal Analysis,Proceedings,11th IAPR International Conference*, pp. 481-484, 1992.

[16] Y. Lee, S. Song, J. Lee, and M. Kim, "Tumor Segmentation from Small Animal

PET using Region Frowing Based on Gradient Magnitude," pp. 243-247, 2005.

[17] P. Felazenszwalb, and D. P. Huttenlocher, "Efficient Graph-Based Image Segmentation," *International Journal of Computer vision*, vol 59, pp. 167-181, 2004.

[18] J. Ashburner, and K. J. Friston, "Image Segmentation," vol 15, pp. 433-438, 2008.

[19] CH. H. Hoi, and M. R. Lyu, " novel log based relevance feedback technique in content based image retrival," *Proceedings of thhe12th annual ACM international conference on Multimedia*, pp. 24-31, 2004.

[20] XS. Zhung, and TS. Huang, "Relevance Feedback in Image Retrival: A Comprehensive Review," vol 8, no. 6, pp. 536-544, 2003.

[21] D. Melas, and S. Wilson, "Double Markov Random Fields and Bayesian Image Segmentation," *Signal Processing, IEEE Transactions*, vol 50, no. 2, pp. 357-365, 2002.

[22] Q. Zhang, SA. Goldman, W. Yu, and JE. Fritts, "Content Based Image Retrival using Multiple Instance Learning," pp. 682-689, 2002.

[23] H. Min, S. Bo, and X. Jianqing, "An Optimized Image Retrival Method Based on Hierarchical Clustering and Generic Algorithm," vol 01, pp. 747-749, 2001.

[24] P. Arbelaez, M. Maire, and C. Fowalkes, "Contour Detection and Hierarchical Image Segmentation," *Pattern Analysis and Machine Intelligence, IEEE Transactions,* vol 33, pp. 898-916, 2011.

[25] JZ. Wang, J. Li, and G. Wierderhold, "Semantics-Sensitive Integrated Matching for Picture Libraries," *Pattern Analysis and Machine Intelligence, IEEE Transactions,* vol 23, no. 9, pp. 947-963, 2001.

[26] J. Shi, and J. Malik, "Normalized cuts and Image Segmentation," *Pattern Analysis and Machine Intelligence,IEEE Transactions,* pp. 888-905, 2010.

[27] J. Shi, and J. Malik, "Motion Segmentation and Tracking using Normalized cuts," *Computer Vision,1998, sixth International Conference,* pp.1154-1160,

1998.

[28] W. Li, Z. Yong, and X. Shixiong, "A Novel Clustering Algorithm Based on Hierarchical and K-Means Clustering," *Control Conference, 2007, Chinese*, pp. 605-609, 2009.

[29] N. Isa, SA. Salamah, and UK. Ngah, "Adaptive Fuzzy Moving K-Means Clustring Algorithm for Image Segmentation," *Consumer Electronics,IEEE Tansactions*, vol 55, no. 4, pp. 2145-2153, 2009.

[30] "Learning," http://www.learningace.com/cs525/ 2002-spring-cs525-lecture-2, pp.21-26,2002.

[31] Chuang, K. Tzeng, S. Chen, J. Wu, and T. Chen, "Fuzzy c-Means Clustering with Spatial Information for Image Segmentation," *Computerized Medical Imaging and Graphics*, vol 30, no. 1, pp. 9-15, 2005.

[32] JC. Bezdek, R. Ethrlich, and W. Full, "FCM: The Fuzzy c-Means Clustering Algorithm," *Computers & Geoscience*, vol 10, no. 2-3, pp. 191-203, 1984.

[33] F. Masulli, and A. Schenone, "A Fuzzy Clustering Based Segmentation System as Support to Diagnosis in Medical Imaging," *Artifitial Intelligence in Medicine,* vol 16, no. 2, pp. 129-147, 1999.

[34] M. C. J. Christ, and R. M. S. Parvathi, "Fuzzy C-Means Algorithm for Medical Image Segmentation," *Electronics Computer Technology(ICECT),2011 3rd International Conference*, 2011.

[35] JC. Bezdek, LO. Hall, LP. Clarke, and RP. Velthuizen, "Review of Image Segmentation Techniques using Pattern Recognition," *Medical Physics*, vol 20, no. 14, pp. 1033-1048, 1993.

[36] "A Totorial on Clustering Algorithm,". Retreieved in June 2011: //home.deib.polimi.it/matteucc/Clustering/tutorial_html/cmeans.html.

[37] Cattin, and Philippe, "Introduction to Signal and Image Processing," vol 32, pp.524-530, 2012.

[38] L. H. Jung, and M. N. Wu, "MRI Brain Image Detection Based on Color-Converted K-Means Clustering Segmentation," *Measurement*, vol 43, no. 7, pp.

941-949, 2010.

[39] X. Zhou, CH. Zhang, and S. Li, "A preceptive uniform pseudo-color coding method of SAR images," *IEEE Transactions,* pp. pp.1-2, 2006.

[40] RC. Gonzalez, and RE. Woods, "Digital Image Processing," second edition, Prenti-Hall,Englewood Cliffs,NJ, pp.116-123, 2002.

[41] CAO. Mao-yong, and Y. Dao-yin, "Pseudocolor Coding of Gray Image Information Content on Gray-Scale Resolution," *IEEE Transactions on Pattern Analysis and Machine Intelligence,* pp. pp.153-155, 2000.

[42] J. Gomes, and L. Velho, "Image processing for computer graphics," *Springer Verlag,* pp. pp83-106, 1997.

[43] V. Mlynarik, S. Gruber, and E. Moser, "Proton T1 and T2 Relaxation Times of Human Brain Metabolites at 3 Tesla," *NMR IN BIOMEDICINE,* pp. 325-331, 2001.

[44] "brainweb," Retrieved in July, www.brainweb.bic.mni.mcgill.ca, 2010.

[45] "NITRC," Retrieved in Septamber, www.nitrc,org,2011.

[46] "promis12," Retreievd in Mars, www.promis12.grand-challenge.org,2012.

[47] S. Rahnamayan, and Z. S. Mohamad, "Tissue Segmentation in Medical Image Based on Image Processing Chain Optimization," vol 18, no 2, pp.107-112, 2010.

[48] Y. Yong, and SH. Huang, "Image Segmentation by Fuzzy C-Means Clustering algorithm with a novel penalty term," *Computing and informatics (Bratislava, Slovakia)*, vol 26, pp. 17-31, 2012.

[49] A. Hore, and D. Ziou, "Image Quality metrics: PSNR vs. SSIM," *Pattern Recognition(ICPR),2010 20th International Conference*, pp. 2366-2369.

[50] N. Rajini, and R. Bhavani, "Automatic MR Brain Tumor Detection using Possibilistic C-Means and K-Means Clustering with color Segmentation," vol

23, pp.74-80, 2012.

[51] KS. Chuang, HL. Tzeng, S. Chen, J. Wu, and TJ. Chen, "Fuzzy c-Means Clustering with Spatial Information for Image Segmentation," *Computerized Medical Imaging and Graphics*, vol 30, no. 1, pp. 9-15, 2005.

[52] C. Carson, S. Belongie, H. Greenspan, and J. Blobworld, "Image Segmentation using Expectation-maximization and its application to image querying," *Digital Object Identifier*, vol 24, no. 8, pp. 1026-1038, 2002.